FEBS Letters 583 (2009) 2882–2886

ELSEVIER

FEBS Letters

journal homepage: www.FEBSLetters.org

Glucose induces FGF21 mRNA expression through ChREBP activation in rat hepatocytes

Katsumi Iizuka [a,b], Jun Takeda [a], Yukio Horikawa [a,b,*]

[a] Department of Diabetes and Endocrinology, Gifu University, Graduate School of Medicine, Gifu 501-1194, Japan
[b] Laboratory of Medical Genomics, The Institute for Molecular and Cellular Regulation, Gunma University, Maebashi-shi 371-8512, Japan

ARTICLE INFO

Article history:
Received 7 May 2009
Revised 27 July 2009
Accepted 29 July 2009
Available online 4 August 2009

Edited by Robert Barouki

Keywords:
Fibroblast growth factor 21
Carbohydrate response element binding protein
Rat hepatocyte
Liver type pyruvate kinase
Fatty acid synthase

ABSTRACT

Fibroblast growth factor 21 (FGF21) has beneficial effects of improving the plasma glucose and lipid profiles in diabetic rodents. Here, we investigated carbohydrate response element binding protein (ChREBP) involvement in the regulation of FGF21 mRNA expression in liver. Glucose stimulation and adenoviral overexpression of dominant active ChREBP increased FGF21 mRNA. Consistently, adenoviral expression of dominant negative Mlx inhibited glucose induction of FGF21 mRNA. Furthermore, deletion studies of mouse FGF21 gene promoter (−2000 to +65 bp) revealed a glucose responsive region between −74 and −52 bp. These findings suggest that FGF21 expression is regulated by ChREBP.

1. Introduction

Fibroblast growth factor 21 (FGF21) belongs to the fibroblast growth factor (FGF) family involved in cell growth, cell differentiation, and embryonic development [1]. FGF21 has been found to have multiple beneficial effects in treatment of metabolic syndrome including obesity as well as diabetes mellitus [2]. Transgenic mice with FGF21 overexpression are resistant to diet-induced obesity and glucose intolerance [3]. Treatment with FGF21 induces energy expenditure and improves glucose intolerance, hypertriglycemia and hepatic steatosis in ob/ob mice [4]. In human, serum FGF21 levels in diabetic or obese individuals are higher than normal, and are significantly correlated with adiposity, plasma fasting insulin and the triglyceride concentration [5]. Furthermore, Akt signaling and PPAR- increases FGF21 mRNA expression in muscle and adipose tissue, respectively [6]. These findings suggest that FGF21 is increased in adaptation to increased body weight and energy intake.

We have reported that ChREBP, a glucose activated transcription factor, regulates lipogenic enzyme gene expression and is involved in the development of metabolic syndrome [7,8]. Transactivity of ChREBP is increased in genetically obese mice, and gene deletion of ChREBP improves metabolic disorders such as fatty liver and glucose intolerance [9]. Recently, some groups have reported that overexpression of dominant negative Mlx, which forms a heterodimer with ChREBP, inhibits glucose mediated FGF21 gene expression in rat hepatocytes [10]. These findings suggest that glucose activation of ChREBP might be involved in FGF21 mRNA expression.

In this study, we tested whether glucose stimulation or activation of ChREBP could increase FGF21 mRNA expression in rat hepatocytes We also performed a deletion study of mouse FGF21 gene promoter and identified the glucose responsive region. Our findings demonstrate that glucose stimulation via ChREBP activation induces FGF21 gene expression in rat primary hepatocytes and that FGF21 has an important role in glucose and lipid homeostasis.

2. Materials and methods

2.1. Materials, tissue materials, hepatocyte isolation, and Taqman PCR analysis

The protocols for all animal experiments were approved by the Institutional Animal Care and Use Committee of Gunma University

Abbreviations: FGF21, fibroblast growth factor 21; ChREBP, cabohydrate response elemnt binding protein; LPK, liver type pyruvate kinase; FASN, fatty acid synthase

* Corresponding author. Address: Department of Diabetes and Endocrinology, Division of Molecule and Structure, Gifu University, Graduate School of Medicine, Gifu 501-1194, Japan. Fax: +81 58 230 6376.
E-mail address: yhorikaw@gifu-u.ac.jp (Y. Horikawa).

0014-5793/$36.00 © 2009 Federation of European Biochemical Societies. Published by Elsevier B.V. All rights reserved.
doi:10.1016/j.febslet.2009.07.053

Medical School (code nos. 08-025 and 08-026). Rat primary hepatocytes were isolated and cultured from 6 weeks age male Wistar rats (SLC) as previously described [11,12].

2.2. Construction of plasmid and adenovirus vectors

pcDNA-daChREBP, Ad-daChREBP, Ad-dnMlx, and pGL4 TK RLuc were used previously [11,12]. The series of pGL3-mFGF21 vectors were constructed as follows: a fragment representing −2000, −1205, −1012, −797, −317, −197, −100, −67, and −40 bp (position −2000/+65, −1205/+65, −1012/+65, −797/+65, −317/+65, −197/+65, −100/+65, −67/+65, and −40/+65 relative to the transcription start site of mouse FGF21 of the native 5′ sequence flanking the mouse FGF21 gene were cloned upstream of the luciferase gene in pGL3 basic vector. The series of pGL3 promoter mFGF21 vectors were constructed as follows: a fragment representing −100/−30, −90/−40, −67/−30, −100/−67 bp (position −100/−30, −90/−40, −67/−30, −100/−67 relative to the transcription start site of mouse FGF21 gene, respectively) of the native 5′ sequence flanking the mouse FGF21 gene were cloned upstream of TK promoter in pGL3 promoter vector. A fragment 3XFGF21 E1(−101/−80 bp) or 3XFGF21 E2 (−74/−52 bp) was cloned upstream of TK promoter in pGL3 promoter vector. Mouse FGF21 cDNA expressing adenovirus (Ad-FGF21) was constructed as follows: Mouse FGF21 full-length cDNA was cloned using Prime Star DNA polymerase reagents. PCR fragment was ligated into pENTR vector (Invitrogen). Recombination of adenovirus and pENTR FGF21 vector was performed to produce Ad-FGF21 vectors according to manufacture's protocol. All plasmid and adenovirus vectors were verified by sequencing analysis.

2.3. Treatment with recombinant adenovirus in rat hepatocytes

Rat primary hepatocytes were cultured in six-well plates in 2 ml DMEM medium. After 2, 10, and 50 m.o.i. of adenovirus bearing GFP, dominant active ChREBP (daChREBP) dominant negative Mlx (dnMlx), or FGF21 was infected into hepatocytes for 2 h, media were removed and infected hepatocytes were incubated in media with 2.5 or 25 mM glucose concentration for 18 h. Cells were then collected and used for RNA extraction, cDNA synthesis and RT-PCR analysis as previously described [11,12].

2.4. Mammalian transfection and reporter assay

Rat primary hepatocytes were cultured in six-well plates in 2 ml DMEM without antibiotics. The cells were transfected with Lipofectamine2000 (10 μl), the series of pGL3-mFGF21 (3.6 μg), and the pGL4 TK RLuc vector (0.4 μg) [12]. After 24 h of incubation at 2.5 or 25 mM glucose concentration, the cells were collected and used to measure luciferase activity (Dual Luciferase assay system; Promega, Madison, WI) according to manufacture's protocol. To determine glucose dependency on the glucose response region in mouse FGF21 gene promoter, cells were transfected with 3.1 μg of pGL3 promoter 3XFGF21 E1, 3XFGF21 E2, or 3XLPK ChoRE vectors, 0.4 μg of pGL4-RLuc-TK vectors and 0.5 μg of pcDNA6.2 empty vector or daChREBP vector. After 24-h incubation with various glucose concentrations, the cells were collected for measurement of luciferase activity.

2.5. Data presentation and statistical methods

All data are expressed as means ± S.D. The listed n values represent the number of single experiments performed (each experiment was duplicated). Comparisons between two groups were performed by student t-test and comparison between multiple groups was performed by Tukey–Kramer test. A value of $P < 0.05$ was regarded as significant.

3. Results

3.1. The role of ChREBP in glucose mediated FGF21 gene expression

As FGF21 mRNA is expressed mainly in islets and liver (Fig. S1A), we examined FGF21 mRNA expression in liver of diabetic model mice. FGF21 mRNA levels in 6 weeks age male STZ mice and ob/ob mice were 1.1- and 2.5-fold higher than that in 6 weeks age C57BL/6J mice, respectively (Fig. S1B). To verify that glucose increased FGF21 mRNA expression, we examined the effect of glucose and ChREBP on FGF21 mRNA expression. High glucose stimulation increased FGF21 mRNA expression in a time dependent manner (Fig. 1A). These findings suggest that a metabolite in the glycolytic and pentose pathway induces FGF21 mRNA expression. Adenoviral overexpression of daChREBP increased FGF21 mRNA expression in a dose-dependent manner (Fig. 1B). Furthermore, Mlx is an obligate heterodimer partner of ChREBP that is required for binding and activation of glucose-regulated gene expression [11]. In accord with Fig. 1B, dnMlx successfully inhibited glucose induction of FGF21 mRNA gene expression in rat primary hepatocytes (Fig. 1C). Similarly, siRNA against ChREBP inhibited not only ChREBP mRNA but also glucose mediated FGF21, liver type pyruvate (LPK), and fatty acid synthase (FASN) gene expression in rat primary hepatocytes (Fig. S1C). Thus, transactivation of ChREBP induces FGF21 mRNA expression in hepatocytes.

3.2. Identification of glucose response region in mouse FGF21 gene promoter

Deletion studies of mouse FGF21 gene promoter showed that a region between −100 and −67 bp is critical for the glucose response to FGF21 mRNA induction (Fig. 2A). We tested in detail putative glucose response elements in mouse FGF21 promoter (between −200 and +0 bp) (Fig. 2B). Fig. 2B shows that a region between −90 and −40 bp is critical for the glucose response to FGF21 mRNA expression. We also determined which putative E-Box (E1: −101/−80 bp and E2: −74/−52 bp) functions as the glucose response element (Supplementary Fig. S2). In accord with Fig. 2A and B, the E2 element (−74/−52 bp) is shown to possesses glucose responsiveness or ChREBP mediated activation of FGF21 mRNA expression (Fig. 2C). We also tested the glucose response to luciferase activity in pGL3-3XFGF21 E2 vector. Compared with pGL3 FGF21 −2 kbp vector, luciferase activities were similarly dependent on the glucose concentration (Fig. 2D).

3.3. Effect of FGF21 overexpression on ChREBP and expression of its target genes in rat hepatocytes

FGF21 lowers plasma glucose and increases glucose uptake in muscle and adipose tissue, but its role in liver is unclear. Because the FGF21 signaling cascade requires both FGF receptors (FGFRs) and beta-Klotho [13,14], we confirmed that all of the FGFRs were present in both mouse liver and rat hepatocytes and beta-Klotho was detected in mouse livers (Fig. S3A and B) [14]. We then tested whether FGF21 affects glucose mediated LPK and FASN mRNA expression in rat hepatocytes. Glucose induction of LPK and FASN mRNA expression in rat hepatocytes infected in a dose-dependent manner with Ad-FGF21 were unchanged as compared with those in untreated hepatocytes (Fig. 3).

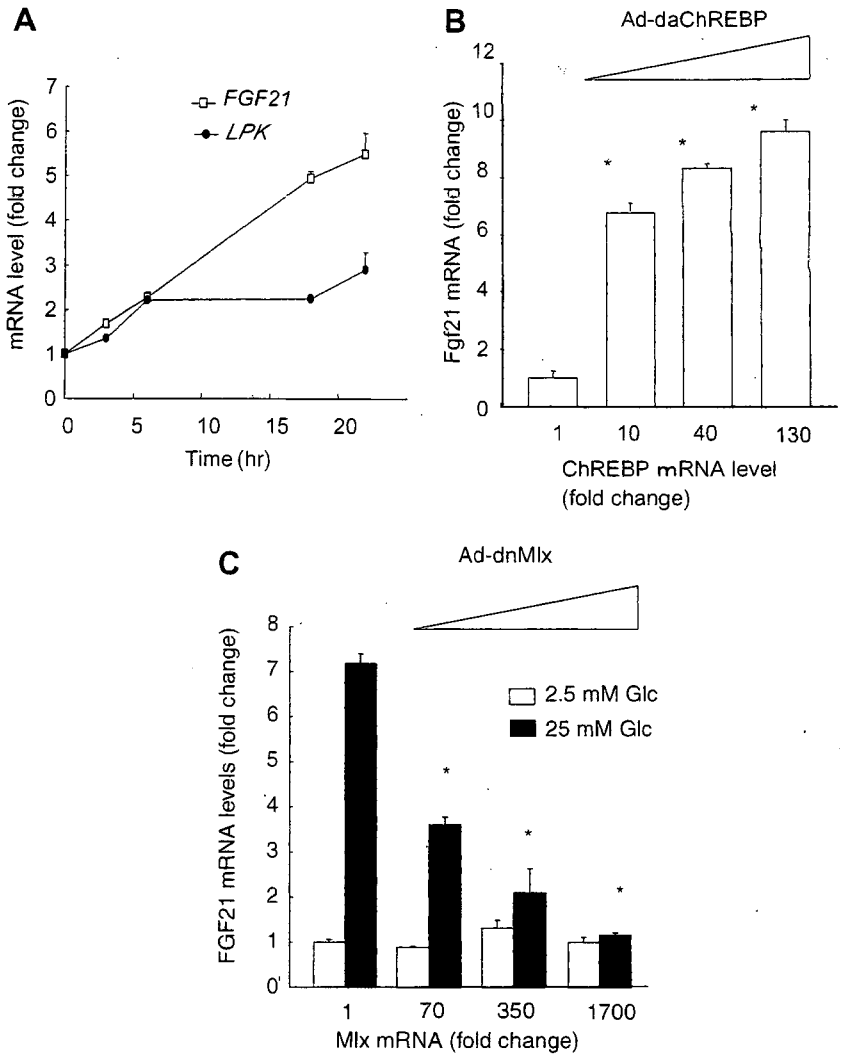

Fig. 1. (A) Glucose stimulates increased FGF21 mRNA expression in rat hepatocytes. Isolated hepatocytes were cultured in Dulbecco's modified Eagle's medium (DMEM) including several concentrations of glucose for 24 h and collected at the indicated hours for Taqman RT-PCR analysis. (B) Adenoviral overexpression of dominant active ChREBP increased FGF21 mRNA expression in rat hepatocytes. Isolated hepatocytes were infected with 2, 10, and 50 m.o.i. of Ad-daChREBP for 2 h. After culture in DMEM with 2.5 mM glucose concentration for 18 h, the cells were collected for Taqman RT-PCR analysis. Data represent means ± S.D. (C) Adenoviral overexpression of dominant negative Mlx increased FGF21 mRNA expression in rat hepatocytes. Isolated hepatocytes were infected with 2, 10, and 50 m.o.i. of Ad-dnMlx for 2 h. After culture in DMEM with 2.5 or 25 mM glucose concentration for 18 h, the cells were collected for Taqman RT-PCR analysis. Values represent means ± S.D. At most points, the error bars are too small to be shown.

4. Discussion

In this study, we show that FGF21 is a target gene of ChREBP in rat primary hepatocytes. Moreover, we identified a glucose response region located between −74 and −52 bp in the FGF21 promoter. Adenoviral delivery of FGF21 cDNA into rat primary hepatocytes was found not to directly affect glucose induction of LPK and FASN mRNA expression in rat hepatocytes. Thus, FGF21 is directly regulated by the glucose activated transcription factor ChREBP, and ChREBP is not directly regulated by FGF21.

As found in a previous study, FGF21 mRNA is most abundant in mouse islets and liver, in which ChREBP is also highly expressed (Fig. S1A) [2,15]. FGF21 mRNA is more highly upregulated in ob/ob mice, but is only slightly induced in STZ mice (Fig. S1B). In addition, ob/ob mice show hyperinsulinemia and hyperglycemia, while STZ mice show hypoinsulinemia and hyperglycemia (Fig. S1B). Considered together with our previous finding that ChREBP activation requires insulin action, glucose-stimulated FGF21 mRNA expression may well require insulin action [12,16]. In accord with the data shown in Fig. 1A, overexpression of daChREBP induced FGF21 mRNA expression and overexpression of dnMlx inhibited glucose-induced FGF21 mRNA expression (Fig. 1B and C). Moreover, siRNA against ChREBP suppressed glucose induction of FGF21 mRNA expression in rat primary hepatocytes (Fig. S1C). These findings indicate that glucose activation of ChREBP induces hepatic FGF21 mRNA expression. In fact, some groups have reported that plasma FGF21 concentrations and hepatic FGF21 mRNA expression in obese and diabetic animal models are much higher than those in control lean animals [5]. ChREBP is remarkably activated in livers from these diabetic animals, further suggesting that glucose activation of ChREBP induces FGF21 mRNA expression. Moreover, satiety signaling such as PPAR- and Akt signaling induces FGF21 mRNA expression [6,16–18]. Thus, FGF21 gene expression is regulated by satiety signals such as glucose and insulin.

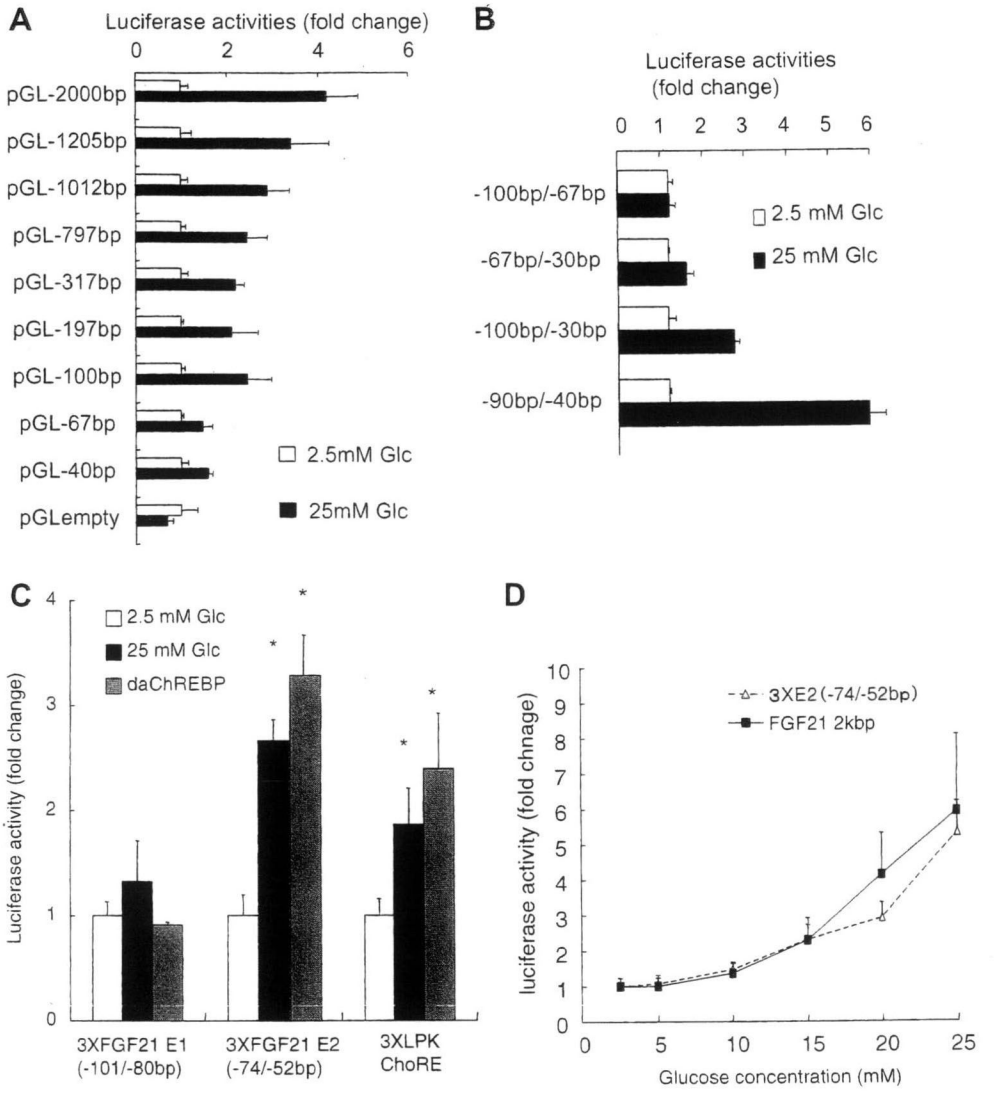

Fig. 2. (A) Deletion studies of mouse FGF21 gene promoter. Isolated hepatocytes were cultured in six-well dishes and transfected with the series of pGL3-mFGF21 vector (3.6 μg) and pGL4 TK RLuc (0.4 μg) using Lipofectamine2000 (10 μl). After 24 h incubation in DMEM including 2.5 or 25 mM glucose concentrations, luciferase activities were measured using Dual Luciferase assay kit. (B) Detailed analysis of the carbohydrate response region in mouse FGF21 promoter. Cells were transfected with the series of pGL3 promoter mFGF mutants (3.6 μg), and pGL4 TK RLuc (0.4 μg) using Lipofectamine2000 (10 μl). After 24 h incubation in DMEM including 2.5 or 25 mM glucose concentrations, luciferase activities were measured using Dual Luciferase assay kit. (C) Reporter analysis of pGL3 promoter 3XFGF21 E2 (−74/−52 bp). Rat primary hepatocytes were transfected with 3.1 μg of pGL3 promoter 3XFGF21 E2 (−74/52p), 3XFgf21 E1 (−101/−80 bp), or 3XLPK ChoRE vectors, 0.4 μg of pGL4-RLuc-TK vectors and 0.5 μg of pcDNA6.2 empty vector or pcDNA6.2 daChREBP vector. Cells were incubated at 2.5 or 25 mM glucose for 24 h and collected for the measurement of luciferase activities. (D) Glucose dependent activation of pGL3 promoter 3XFGF21 E2 (−74/−52 bp) vector and pGL3-mFGF21 −2 kbp. Cells were transfected with 3.6 μg of pGL3 promoter 3XFGF21 E2 (−74/−52 bp) vector or pGL3-mFGF21 −2 kbp and 0.4 μg of pGL4-RLuc-TK vector. Cells were incubated at several glucose concentrations for 24 h and collected for measurement of luciferase activities. Values represent means ± S.D. At most points, the error bars are too small to be shown. $^{*}P < 0.05$ vs. Ad-GFP.

It has been reported that administration of FGF21 in livers of diet-induced obese mice reduces hepatic ChREBP-target gene expression [4,19]. The FGF21 signaling cascade requires the FGF21 receptor complex, FGFR, and an adapter-like molecule, beta-Klotho [14]. Beta-Klotho and FGFR1-4 are abundantly expressed in liver, adipose tissues, and pancreas [14,15,20–22]. In our experiments, all FGFRs were detectable in mouse liver and rat hepatocytes and beta-Klotho was detected only in mouse liver (Fig. S3A and B). The sequence of rat beta-Klotho cDNA remains unknown and we could not check beta-Klotho mRNA expression in rat primary hepatocytes. We then tested whether FGF21 directly affects glucose activation of ChREBP-target gene expressions such as LPK and FASN. We found that FGF21 had no significant effects on the expression of these genes in rat hepatocytes (Fig. 3). GLUT1 gene expression, an FGF21 target, was also unchanged in rat hepatocytes infected by Ad-FGF21 (data not shown). Consistent with these data, some groups have reported that FGF21 does not act on mouse primary hepatocytes and rat hepatoma cell lines, even in the presence of beta-Klotho and FGFRs [14,23,24]. In contrast, some groups reported the opposite evidences that FGF21 is active in cells of hepatic origin [25]. The presence of beta-Klotho in rat primary hepatocytes remains unknown and it will be needed to further investigate the direct action of FGF21 in liver. In conclusion, these results indicate that FGF21 suppresses ChREBP transactivity at least indirectly by lowering plasma glucose concentrations in the whole body.

In conclusion, glucose induces FGF21 mRNA expression via transactivation of ChREBP, indicating that both FGF21 and ChREBP are involved in the regulation of glucose and lipid homeostasis in liver. Thus, FGF21 may well be a useful drug in the treatment of diabetes and obesity.

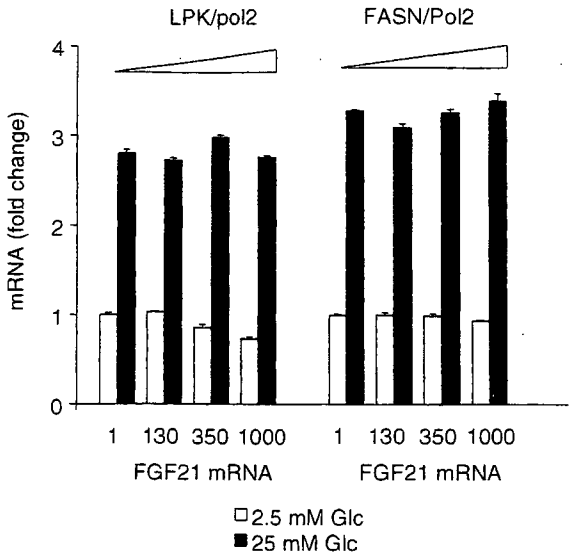

Fig. 3. Adenoviral overexpression of FGF21 did not inhibit LPK and FASN mRNA. Adenovirus expressing either GFP or FGF21 was transduced into rat hepatocytes at m.o.i. of 2, 10, and 50. As control, recombinant adenovirus expressing GFP was used at m.o.i. of 50. Two h after infection, the cells were cultured in DMEM including 2.5 or 25 mM glucose for an additional 18 h. Total RNA was extracted from hepatocytes, and RT-PCR analysis was performed. Values represent means ± S.D. At most points, the error bars are too small to be shown.

Acknowledgments

This work was supported by Grants-in-Aid for Scientific Research from the Japan Society for the Promotion of Science (K. Iizuka), a New Energy and Industrial Technology Development Organization grant (Y. Horikawa), a Health and Labor Science Research Grant for Research on Human Genome (J. Takeda) and Tissue Engineering from the Japanese Ministry of Health, Labor and Welfare, the ONO Medical Research Foundation (K. Iizuka), and the Kao Research Council for the Study of Healthcare Science (K. Iizuka).

Appendix A. Supplementary data

Supplementary data associated with this article can be found, in the online version, at doi:10.1016/j.febslet.2009.07.053.

References

[1] Nishimura, T., Nakatake, Y., Konishi, M. and Itoh, N. (2000) Identification of a novel FGF, FGF-21, preferentially expressed in the liver. Biochim. Biophys. Acta 1492, 203–206.
[2] Kharitonenkov, A. and Shanafelt, A.B. (2008) Fibroblast growth factor-21 as a therapeutic agent for metabolic diseases. BioDrugs 22, 37–44.
[3] Kharitonenkov, A., Shiyanova, T.L., Koester, A., Ford, A.M., Micanovic, R., Galbreath, E.J., Sandusky, G.E., Hammond, L.J., Moyers, J.S., Owens, R.A., Gromada, J., Brozinick, J.T., Hawkins, E.D., Wroblewski, V.J., Li, D.S., Mehrbod, F., Jaskunas, S.R. and Shanafelt, A.B. (2005) FGF-21 as a novel metabolic regulator. J. Clin. Invest. 115, 1627–1635.
[4] Coskun, T., Bina, H.A., Schneider, M.A., Dunbar, J.D., Hu, C.C., Chen, Y., Moller, D.E. and Kharitonenkov, A. (2008) Fibroblast growth factor 21 corrects obesity in mice. Endocrinology 149, 6018–6027.
[5] Zhang, X., Yeung, D.C., Karpisek, M., Stejskal, D., Zhou, Z.G., Liu, F., Wong, R.L., Chow, W.S., Tso, A.W., Lam, K.S. and Xu, A. (2008) Serum FGF21 levels are increased in obesity and are independently associated with the metabolic syndrome in humans. Diabetes 57, 1246–1253.
[6] Muise, E.S., Azzolina, B., Kuo, D.W., El-Sherbeini, M., Tan, Y., Yuan, X., Mu, J., Thompson, J.R., Berger, J.P. and Wong, K.K. (2008) Adipose fibroblast growth factor 21 is up-regulated by peroxisomeproliferator-activated receptor gamma and altered metabolic states. Mol. Pharmacol. 74, 403–412.
[7] Iizuka, K., Bruick, R.K., Liang, G., Horton, J.D. and Uyeda, K. (2004) Deficiency of carbohydrate response element-binding protein (ChREBP) reduces lipogenesis as well as glycolysis. Proc. Natl. Acad. Sci. USA 101, 7281–7286.
[8] Iizuka, K. and Horikawa, Y. (2008) ChREBP: a glucose-activated transcription factor involved in the development of metabolic syndrome. Endocr. J. 55, 617–624.
[9] Iizuka, K., Miller, B. and Uyeda, K. (2006) Deficiency of carbohydrate-activated transcription factor ChREBP prevents obesity and improves plasma glucose control in leptin-deficient (ob/ob) mice. Am. J. Physiol. Endocrinol. Metab. 291, E358–364.
[10] Ma, L., Robinson, L.N. and Towle, H.C. (2006) ChREBP*Mlx is the principal mediator of glucose-induced gene expression in the liver. J. Biol. Chem. 281, 28721–28730.
[11] Iizuka, K., Takeda, J. and Horikawa, Y. (2009) Hepatic overexpression of dominant negative Mlx improves metabolic profile in diabetes-prone C57BL/6J mice. Biochem. Biophys. Res. Commun. 379, 499–504.
[12] Iizuka, K. and Horikawa, Y. (2008) Regulation of lipogenesis via BHLHB2/DEC1 and ChREBP feedback looping. Biochem. Biophys. Res. Commun. 374, 95–100.
[13] Kharitonenkov, A., Dunbar, J.D., Bina, H.A., Bright, S., Moyers, J.S., Zhang, C., Ding, L., Micanovic, R., Mehrbod, S.F., Knierman, M.D., Hale, J.E., Coskun, T. and Shanafelt, A.B. (2008) FGF-21/FGF-21 receptor interaction and activation is determined by beta-Klotho. J. Cell Physiol. 215, 1–7.
[14] Kurosu, H., Choi, M., Ogawa, Y., Dickson, A.S., Goetz, R., Eliseenkova, A.V., Mohammadi, M., Rosenblatt, K.P., Kliewer, S.A. and Kuro-o, M. (2007) Tissue-specific expression of beta-Klotho and fibroblast growth factor (FGF) receptor isoforms determines metabolic activity of FGF19 and FGF21. J. Biol. Chem. 282, 26687–26695.
[15] Wente, W., Efanov, A.M., Brenner, M., Kharitonenkov, A., Köster, A., Sandusky, G.E., Sewing, S., Treinies, I., Zitzer, H. and Gromada, J. (2006) Fibroblast growth factor-21 improves pancreatic beta-cell function and survival by activation of extracellular signal-regulated kinase 1/2 and Akt signaling pathways. Diabetes 55, 2470–2478.
[16] Izumiya, Y., Bina, H.A., Ouchi, N., Akasaki, Y., Kharitonenkov, A. and Walsh, K. (2008) FGF21 is an Akt-regulated myokine. FEBS Lett. 582, 3805–3810.
[17] Wang, H., Qiang, L. and Farmer, S.R. (2008) Identification of a domain within peroxisome proliferator-activated receptor gamma regulating expression of a group of genes containing fibroblast growth factor 21 that are selectively repressed by SIRT1 in adipocytes. Mol. Cell. Biol. 28, 188–200.
[18] Moyers, J.S., Shiyanova, T.L., Mehrbod, F., Dunbar, J.D., Noblitt, T.W., Otto, K.A., Reifel-Miller, A. and Kharitonenkov, A. (2007) Molecular determinants of FGF-21 activity-synergy and cross-talk with PPARgamma signaling. J. Cell Physiol. 210, 1–6.
[19] Xu, J., Lloyd, D.J., Hale, C., Stanislaus, S., Chen, M., Sivits, G., Vonderfecht, S., Hecht, R., Li, Y.S., Lindberg, R.A., Chen, J.L., Jung, D.Y., Zhang, Z., Ko, H.J., Kim, J.K. and Véniant, M.M. (2009) Fibroblast growth factor 21 reverses hepatic steatosis, increases energy expenditure, and improves insulin sensitivity in diet-induced obese mice. Diabetes 58, 250–259.
[20] Arner, P., Pettersson, A., Mitchell, P.J., Dunbar, J.D., Kharitonenkov, A. and Rydén, M. (2008) FGF21 attenuates lipolysis in human adipocytes - a possible link to improved insulin sensitivity. FEBS Lett. 582, 1725–1730.
[21] Ito, S., Kinoshita, S., Shiraishi, N., Nakagawa, S., Sekine, S., Fujimori, T. and Nabeshima, Y.I. (2000) Molecular cloning and expression analyses of mouse betaklotho, which encodes a novel Klotho family protein. Mech. Dev. 98, 115–119.
[22] Lin, B.C., Wang, M., Blackmore, C. and Desnoyers, L.R. (2007) Liver-specific activities of FGF19 require Klotho beta. J. Biol. Chem. 282, 27277–27284.
[23] Inagaki, T., Lin, V.Y., Goetz, R., Mohammadi, M., Mangelsdorf, D.J. and Kliewer, S.A. (2008) Inhibition of growth hormone signaling by the fasting-induced hormone FGF21. Cell Metab. 8, 77–83.
[24] Kurosu, H. and Kuro-O, M. (2009) The Klotho gene family as a regulator of endocrine fibroblast growth factors. Mol. Cell Endocrinol. 299, 72–78.
[25] Kharitonenkov, A. and Shanafelt, A.B. (2009) FGF21: a novel prospect for the treatment of metabolic diseases. Curr. Opin. Investig. Drugs 10, 359–364.

DIABETES RESEARCH AND CLINICAL PRACTICE 85 (2009) 189–196

Contents lists available at ScienceDirect

Diabetes Research and Clinical Practice

journal homepage: www.elsevier.com/locate/diabres

Associations of coronary artery calcification and carotid intima-media thickness with plasma concentrations of vascular calcification inhibitors in type 2 diabetic patients

Masami Ishiyama [a], Eiji Suzuki [a,b,*], Jun Katsuda [a], Hiroshi Murase [a], Yoshitaka Tajima [a], Yukio Horikawa [a], Shinobu Goto [c], Tamio Fujita [c], Jun Takeda [a]

[a] Department of Diabetes and Endocrinology, Gifu University School of Medicine, 1-1 Yanagido, Gifu, Gifu 501-1194, Japan
[b] Department of Internal Medicine, Gifu Prefectural General Medical Center, 4-6-1 Noishiki, Gifu, Gifu 500-8717, Japan
[c] Department of Internal Medicine, Nagoya Memorial Hospital, 4-305 Hirabari, Tenpaku-ku, Nagoya 468-8520, Japan

ARTICLE INFO

Article history:
Received 11 September 2008
Received in revised form
19 April 2009
Accepted 28 April 2009
Published on line 3 June 2009

Keywords:
Coronary artery calcification
Carotid intima-media thickness
Bone-related peptide
Type 2 diabetes

ABSTRACT

Vascular calcification is frequently accompanied by intima-media thickening, but the associations among these atherosclerotic features and bone-related peptides in diabetic patients are unclear. We enrolled 168 type 2 diabetic patients and 40 non-diabetic subjects consecutively admitted to our hospital. Mean intima-media thickness (mean-IMT) in common carotid arteries was measured by B-mode ultrasonography. Agatston coronary artery calcium score (CACS) was obtained using multidetector-row computed tomography (MDCT). Plasma bone-related peptides osteopontin and osteoprotegerin levels were measured. Diabetic patients had higher mean-IMT ($p = 0.0002$) and log(CACS + 1) ($p < 0.0001$) and similar bone-related peptides compared to non-diabetic subjects. In diabetic patients classified into tertiles according to their CACS levels, those with the highest scores showed the highest mean-IMT ($p = 0.0004$) and bone-related peptides ($p < 0.05$) among the groups. log(CACS + 1) and mean-IMT were associated ($p < 0.0001$) and were positively correlated with osteopontin ($p < 0.01$) and osteoprotegerin ($p < 0.01$) in diabetic patients. Multivariate analyses revealed that the significant independent determinants of log(CACS + 1) were age, duration of diabetes and osteopontin ($p < 0.0001$) and those of mean-IMT were age, hypertension, osteopontin and osteoprotegerin ($p < 0.0001$), respectively. We have demonstrated that vascular calcification in type 2 diabetic patients is frequently accompanied by intima-media thickening, and osteopontin may act as a vascular calcification inhibitor by increasing intima-media thickness.

1. Introduction

Patients with type 2 diabetes have an increased risk of coronary artery disease (CAD) that is often silent [1]. It is important to detect coronary atherosclerosis before the onset of life-threatening CAD events. Vascular calcification is an essential feature of atherosclerosis that begins early in the atherosclerotic process [2]. A number of studies have investigated the usefulness of ultrafast computed tomography, such as electron-beam computed tomography (EBCT) [3] and multidetector-row

* *Corresponding author at:* Department of Diabetes and Endocrinology, Gifu University School of Medicine, 1-1 Yanagido, Gifu, Gifu 501-1194, Japan. Tel.: +81 58 230 6373; fax: +81 58 230 6375.
E-mail address: esuzuki@gifu-u.ac.jp (E. Suzuki).
0168-8227/$ – see front matter © 2009 Elsevier Ireland Ltd. All rights reserved.
doi:10.1016/j.diabres.2009.04.023

computed tomography (MDCT) [4], for the detection of coronary artery calcification. Calcium deposits in coronary arteries accumulate predominantly in the intimal layer rather than the medial wall [5], and the amount of calcification correlates with the overall burden of atherosclerosis [3]. Measurement of carotid intima-media thickness (IMT) by B-mode ultrasonography is used to assess atherosclerotic involvement in the intimal and medial layers. Scoring of coronary artery calcification [6] and measurement of carotid IMT [7] are powerful predictors of angiographic coronary artery stenoses, and these parameters are increased in diabetic patients [7,8].

Vascular calcification was previously thought to be a passive consequence of chronic vascular inflammation and the degenerative process of atherosclerosis. It is now recognized as a protective response to chronic vascular inflammation, and is an actively regulated process by inductive and inhibitory molecules similar to those involved in bone mineralization. Bone structural proteins and key regulators of bone mineralization such as osteopontin and osteoprotegerin are found in increased amounts in carotid endarterectomy samples taken from stroke patients [9]. Osteopontin is an acidic phosphoprotein normally restricted to bone matrix, and is present focally in calcified atherosclerotic plaques but is absent in non-diseased coronary arteries [10]. Osteopontin is abundantly synthesized by infiltrating macrophages, endothelial cells and vascular smooth muscle cells (VSMCs) in atherosclerotic plaques [11], and inhibits vascular calcification by preventing apatite crystal growth and inducing cellular mineral resorption [12]. Osteoprotegerin is a soluble member of the tumor necrosis factor receptor superfamily, and is produced by osteoblastic cells, endothelial cells and VSMCs [13,14]. Osteoprotegerin inhibits osteoclast functions by neutralizing the receptor activator of NF-κB ligand [15], and exogenous administration of this molecule in rats can inhibit bone resorption and arterial calcification [16]. Plasma osteopontin levels are associated with the numbers of stenotic or calcified segments in patients with CAD [17] and increased risk of cardiovascular events in patients with chronic stable angina [18] assessed by coronary angiography. Circulating osteoprotegerin levels were also associated with the number of diseased vessels in patients with stable chest pain who underwent coronary angiography [19]. However, a small proportion of diabetic patients (25–37%) was included in these studies [17–19]. While plasma osteoprotegerin concentrations are associated with coronary artery calcification score evaluated with EBCT [20] and silent myocardial ischemia using stress myocardial perfusion imaging [21] in type 2 diabetic patients, whether or not vascular calcification is accompanied by intima-media thickening and the associations of these atherosclerotic features with bone-related peptides in diabetic patients are not known.

In the present study, we investigated the association of coronary artery calcium score with carotid IMT and whether or not the atherosclerotic features are associated with plasma osteopontin and osteoprotegerin concentrations in type 2 diabetic patients.

2. Materials and methods

One hundred sixty-eight type 2 diabetic patients and 40 non-diabetic subjects ranging in age from 40 to 75 years who had been consecutively admitted to our hospital between April 2005 and May 2008 were recruited for the study. All patients were admitted for strict glycemic control or assessment of diabetic complications. No patients had clinical history of cerebrovascular disease, CAD, or peripheral artery occlusive disease. Patients who abused alcohol or showed heart failure, liver cirrhosis, severely decreased estimated glomerular filtration rate (eGFR) <30 ml/min per 1.73 m^2, malignant neoplasm, acute illness or urinary tract infections were excluded from the study. Patients were considered to have cerebrovascular disease if they had a history of sudden focal neurological deficit. CAD was diagnosed if the patients had a history of myocardial infarction or showed abnormal electrocardiographic findings. Peripheral arterial occlusive disease was diagnosed if the patients had an abnormal ankle-brachial index (ABI) of <0.9 at rest [22]. Presence of pyuria or hematuria was diagnosed by microscopic examination and counting of the number of white blood cells or red blood cells per high-power field in the last voided urine of a 24 h collection. All diabetic patients with hypertension (>140/90 mmHg) received angiotensin converting enzyme inhibitor (ACEI) or angiotensin II receptor blocker (ARB) for the management of high blood pressure, although administration of these renin-angiotensin system (RAS) inhibitors can decrease the progression of coronary artery calcification [23] and carotid IMT in diabetic patients [24]. Hydroxymethylglutaryl coenzyme A reductase inhibitors (statins) can also reduce the progression of coronary artery calcification [25] and the burden of carotid IMT [26], and were used for the treatment of dyslipidemia (total cholesterol >6.21 mmol/l) in diabetic patients. A 75 g glucose tolerance test was performed in our outpatient clinic to determine if the subjects had normal glucose regulation, impaired glucose tolerance and diabetes mellitus. Individuals with normal glucose tolerance were used as non-diabetic subjects [27]. The study was approved by the ethics committee of our institution, and informed consent was obtained from all subjects before the examinations, which were done during their stay in the hospital.

Blood samples were drawn before breakfast in the morning after a 12 hour overnight fast. Blood pressure was measured by a mercury sphygmomanometer with the patients in the sitting position after 5 min of rest. Three readings separated by 2 min were taken, and the average was used for analysis. An automatic device (BP-203RPE; Colin, Komaki, Japan) was used to measure ABI and brachial-ankle pulse wave velocity (baPWV) as an index of stiffness in elastic and muscular arteries [28]. A trained ophthalmologist carried out fundus ophthalmoscopies and classified diabetic patients without retinopathy or with simple or proliferative retinopathy. Patients with diabetes were screened for distal symmetric polyneuropathy using a 128 Hz tuning fork applied to the bony prominence at the dorsalis surface of both great toes, just proximal to the nail bed [29]. When the tuning fork was placed on the foot, if the patients required >10 s to detect the vibration, vibration perception was regarded as compromised. Diabetic patients were classified by measurement of urinary albumin excretion (UAE) in 24 h urine collection as having normoalbuminuria, microalbuminuria, or macroalbuminuria when at least two of three specimens were at diagnostic thresholds of less than 30, 30–300, or greater than 300 mg/24 h,

respectively [30]. The Japanese ethnic factor for the modification of diet in renal disease (MDRD) equation has been reported to be 0.881 [31]. Therefore, the eGFR was calculated by the MDRD formula as follows: eGFR (ml/min per 1.73 m^2) = $0.881 \times 186.3 \times Age^{-0.203} \times SCr^{-1.154}$ (if female × 0.742), where SCr is serum creatinine (mg/dl). Renal insufficiency was defined as eGFR of <60 ml/min per 1.73 m^2 [32]. Each subject was also classified as a current smoker or non-smoker. Non-smokers were defined as not using tobacco for at least previous 3 years. Plasma concentrations of B-type natriuretic peptide (BNP) were determined using a chemiluminescent enzyme immunoassay kit (MIO2 Shionogi BNP, Shionogi & Co., Ltd., Osaka, Japan). Plasma osteopontin concentrations were determined using enzyme-linked immunosorbent assay kits (Human Osteopontin Assay Kit - IBL, Gunma, Japan). The detection limit of this assay system was 25 ng/ml, and the intra- and inter-assay coefficient of variation values were 8.0% and 4.7%, respectively. Plasma osteoprotegerin concentrations were determined using enzyme-linked immunosorbent assay kits (Human Osteoprotegerin ELISA Kit, Immundiagnostik AG, Bensheim, Germany). The detection limit of this assay system was 7.4 pg/ml, and the intra- and inter-assay coefficient of variation values were 10% and <10%, respectively.

Twenty contiguous slices of 3-mm thickness of the proximal coronary arteries were obtained during a single breath hold using a 16 multidetector-row computed tomography (16-MDCT) scanner (Aquilion 16, Toshiba Medical Systems Corporation, Tokyo, Japan). These scans are electrocardiographically triggered at 70% of the R–R interval, near the end of diastole and before atrial contraction, to minimize the effect of cardiac motion. The severity of coronary artery calcification was analyzed on Ziostation (Amin Co., Ltd., Tokyo, Japan) with scoring software (scoring of coronary artery calcification Version 1.17). The Agatston coronary artery calcium score (CACS), including both intimal and medial calcification in left main, left anterior descending, circumflex and right coronary arteries, was obtained as a quantitative marker of calcium burden in the coronary arteries [33]. Comparison of 16-MDCT and EBCT indicates that 16-MDCT can detect coronary artery calcification and may be an alternative to EBCT [4]. The test results were almost equivalent in coronary artery calcium scoring: 16-MDCT score = 7.7 + 1.015 × EBCT score ($r^2 = 0.955$).

Ultrasonographic scanning of the carotid arteries was performed with a high-resolution duplex ultrasound scanner (EUB-7500; Hitachi Medical Corp., Kashiwa, Japan) and a high-resolution 14–6 MHz broadband linear array transducer for the B-mode scan. Each subject was examined in the supine position with their head turned 45° from the side being scanned. The right and left common carotid arteries were scanned for measurement of IMT in three different longitudinal (anterior-oblique, lateral and posterior-oblique) and transverse views. The image was focused on the far wall of the artery. IMT was defined as the distance between the leading edge of the lumen-intima interface to the leading edge of the media-adventitia interface of the far wall. In each longitudinal projection, three sites, at the greatest thickness and at 1 cm distal and proximal, were averaged and expressed as mean-IMT. The highest value among the six mean-IMTs was used as the representative value for each individual. All measurements were performed by a single trained sonographer who was unaware of the clinical profile of the study subjects. The intraobserver reproducibility of mean-IMT measurement was established by repeating the procedure after 2 weeks in 32 diabetic patients. The mean absolute difference between the two measurements was 0.011 ± 0.060 mm and coefficient of correlation was 0.945 ($p < 0.0001$).

Statistical evaluation was performed on SPSS software version 11.0 for Windows (SPSS Inc., Chicago, IL, USA). Normality of distribution of each variable was assessed with the Kolmogorov–Smirnov test. Comparison between the two groups was performed using the unpaired Student's t-test. A multiple comparison of significant differences among the three groups was carried out by one-way analysis of variance followed by Scheffe's F test. The chi-square test for two-by-two or Bonferroni test for two-by-three contingency table was used to compare frequencies between two groups or among three groups. Pearson's correlation coefficient was applied to assess the relation between normally distributed variables. Since distribution of CACS was highly skewed, common log-transformed CACS [log(CACS + 1)] was used for linear regression analysis. Stepwise multiple regression analyses were performed to evaluate the association of log(CACS + 1) or mean-IMT with 12 possible risk factors for atherosclerosis, two medications and two bone-related peptides in diabetic patients. The F value was set at 4.0 at each step. Values are expressed as the mean ± SD. P values <0.05 were considered to be statistically significant.

3. Results

3.1. All subjects

Clinical characteristics in all subjects are summarized in Table 1. There were no significant differences between the groups for prevalence of male gender, age, body mass index (BMI), total cholesterol (TC), triglycerides (TGs), frequency of smoking habit, eGFR, ABI, serum levels of calcium (Ca), inorganic phosphate (IP) and alkaline phosphatase (ALP) and osteopontin and osteoprotegerin. Diabetic patients had higher fasting plasma glucose (FPG) ($p < 0.0001$), hemoglobin A1c (HbA1c) ($p < 0.0001$), systolic blood pressure (sBP) ($p = 0.0030$), frequency of elevated UAE ($p < 0.0001$) and neuropathy ($p < 0.0001$), mean-IMT ($p = 0.0002$), log(CACS + 1) ($p < 0.0001$), baPWV ($p < 0.0001$) and BNP ($p = 0.0120$) and lower HDL cholesterol (HDL-C) ($p = 0.0002$) and diastolic blood pressure (dBP) ($p = 0.0026$) compared with non-diabetic subjects.

3.2. Coronary artery calcification

To compare the clinical characteristics of diabetic patients with coronary artery calcification, they were classified into tertiles according to their CACS levels. The clinical characteristics of these subgroups are shown in Table 2. There were no significant differences among the groups for prevalence of male gender, BMI, FPG, HbA1c, TC, HDL-C, TGs, frequency of patients taking statins, dBP, prevalence of smoking habit, neuropathy, ABI, Ca, IP, and ALP. Patients in the highest range

Table 1 – Clinical characteristics in diabetic patients and non-diabetic subjects.

	Non-diabetic subjects	Diabetic patients	p-value
Number	40	168	–
Male gender (%)	18 (45.0)	97 (57.7)	0.2008
Age (years)	59.6 ± 6.3	62.1 ± 9.3	0.1048
BMI (kg/m^2)	23.4 ± 3.1	24.3 ± 4.2	0.1896
Duration of diabetes (years)	–	10.0 ± 8.1	–
Treatment (diet/OHD/insulin)	–	18/102/48	–
FPG (mmol/l)	5.54 ± 0.67	7.87 ± 2.78	<0.0001
HbA1c (%)	5.2 ± 0.4	7.6 ± 1.8	<0.0001
TC (mmol/l)	5.39 ± 0.94	5.10 ± 1.13	0.1278
HDL-C (mmol/l)	1.55 ± 0.45	1.27 ± 0.42	0.0002
TGs (mmol/l)	1.42 ± 0.84	1.58 ± 0.74	0.2275
Statins (%)	–	51 (30.4)	–
Blood pressure (mmHg)			
Systolic	125 ± 13	133 ± 16	0.0030
Diastolic	78 ± 10	73 ± 10	0.0026
ACEI or ARB (%)	–	58 (34.5)	–
Smokers (%)	9 (22.5)	62 (36.9)	0.1233
Retinopathy (%)	–	55 (32.7)	–
Micro- or macroalbuminuria (%)	0 (0)	72 (42.9)	<0.0001
eGFR (ml/min per 1.73 m^2)	68.5 ± 7.4	70.7 ± 18.3	0.4565
Neuropathy (%)	0 (0)	52 (31.0)	<0.0001
Carotid mean-IMT (mm)	0.80 ± 0.28	0.98 ± 0.27	0.0002
Log (CACS + 1)	0.60 ± 0.84	1.42 ± 1.18	<0.0001
ABI	1.15 ± 0.07	1.15 ± 0.09	0.9866
Brachial-ankle PWV (cm/s)	1472 ± 243	1752 ± 393	<0.0001
Ca (mmol/l)	2.31 ± 0.08	2.32 ± 0.14	0.6833
IP (mmol/l)	1.14 ± 0.16	1.09 ± 0.17	0.1027
ALP (IU/l)	226 ± 62	236 ± 56	0.3415
BNP (pg/ml)	13.3 ± 15.6	26.5 ± 32.0	0.0120
Osteopontin (ng/ml)	325 ± 136	333 ± 152	0.7383
Osteoprotegerin (pg/ml)	80.8 ± 39.6	87.2 ± 38.0	0.3492

Data are expressed as n (%) or means ± SD. OHD; oral hypoglycemic drugs.

had the highest age ($p < 0.0001$), duration of diabetes ($p = 0.0008$), sBP ($p = 0.0233$), frequency of taking ACEI or ARB ($p < 0.01$), retinopathy ($p < 0.01$), mean-IMT ($p = 0.0004$), baPWV ($p = 0.0002$), BNP ($p = 0.0375$), osteopontin ($p = 0.0294$) and osteoprotegerin ($p = 0.0311$) and the lowest eGFR ($p = 0.0451$) among these groups. To determine if vascular calcification is frequently accompanied by intima-media thickening, simple linear regression analyses were performed as shown in Fig. 1. log(CACS + 1) was positively correlated with mean-IMT ($p < 0.0001$) in diabetic patients.

3.3. *Bone-related peptides*

To clarify the associations of vascular calcification and intima-media thickening with circulating levels of bone-related peptides, simple linear regression analyses were performed as shown in Fig. 2. log(CACS + 1) was positively correlated with osteopontin ($p = 0.0010$) (Fig. 2A) and osteoprotegerin ($p = 0.0027$) (Fig. 2B) and mean-IMT was positively correlated with osteopontin ($p = 0.0030$) (Fig. 2C) and osteoprotegerin ($p = 0.0011$) (Fig. 2D) in diabetic patients, respectively. Stepwise multiple regression analyses were performed as shown in Table 3 to examine the association of log(CACS + 1) or carotid mean-IMT with 12 possible risk factors for atherosclerosis (age, duration of diabetes, FPG, HbA1c, sBP, dBP, TC, HDL-C, TGs, smoking habit, micro- or macroalbuminuria and eGFR), two medications (use of RAS inhibitors or statins) and two bone-related peptides (osteopontin and osteoprotegerin). The significant independent determinants of log(CACS + 1) were age, duration of diabetes and osteopontin ($r^2 = 0.215$,

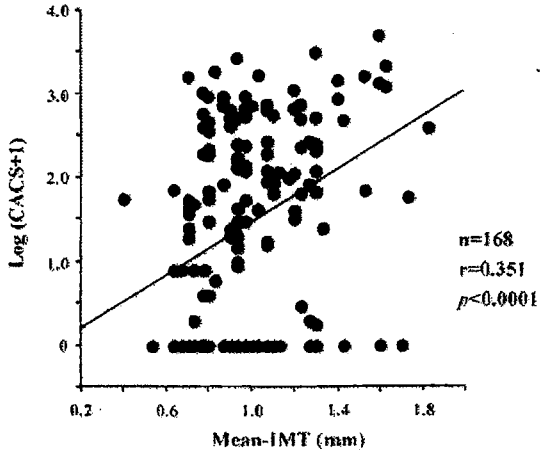

Fig. 1 – Simple linear regression analysis between coronary artery calcium score (CACS) and mean value of intima-media thickness (mean-IMT) in the common carotid arteries in type 2 diabetic patients.

Table 2 – Diabetic patients classified into tertiles based on their levels of Agatston coronary artery calcium score (CACS).

Range of CACS	Lowest group <1.00	Intermediate group 1.00–130	Highest group 133–4956
Number	56	56	56
Male gender (%)	27 (48.2)	35 (62.5)	35 (62.5)
Age (years)	56.6 ± 9.6	64.0 ± 9.2**	66.3 ± 6.9**
BMI (kg/m^2)	24.5 ± 4.9	24.3 ± 3.9	24.1 ± 3.8
Duration of diabetes (years)	7.0 ± 7.2	10.4 ± 7.4	12.7 ± 8.7**
Treatment (diet/OHD/insulin)	7/33/16	6/35/15	5/34/17
FPG (mmol/l)	8.42 ± 2.91	7.43 ± 2.83	7.75 ± 2.55
HbA1c (%)	7.7 ± 1.8	7.7 ± 2.1	7.5 ± 1.6
TC (mmol/l)	5.32 ± 1.32	5.01 ± 1.09	4.96 ± 0.92
HDL-C (mmol/l)	1.27 ± 0.37	1.31 ± 0.54	1.23 ± 0.34
TGs (mmol/l)	1.47 ± 0.81	1.58 ± 0.74	1.68 ± 0.67
Statins (%)	12 (21.4)	18 (32.1)	21 (37.5)
Blood pressure (mmHg)			
Systolic	129 ± 16	132 ± 15	137 ± 15*
Diastolic	72 ± 10	73 ± 11	74 ± 9
ACEI or ARB (%)	10 (17.9)	21 (37.5)	27 (48.2)**
Smokers (%)	22 (39.3)	19 (33.9)	21 (37.5)
Retinopathy (%)	10 (17.9)	18 (32.1)	27 (48.2)**
Micro- or macroalbuminuria (%)	22 (39.3)	21 (37.5)	29 (51.8)
eGFR (ml/min per 1.73 m^2)	75.2 ± 15.5	70.2 ± 22.1	66.6 ± 15.9*
Neuropathy (%)	15 (26.8)	16 (28.6)	21 (37.5)
Carotid mean-IMT (mm)	0.89 ± 0.24	0.96 ± 0.25	1.09 ± 0.28**,†
ABI	1.14 ± 0.08	1.17 ± 0.08	1.14 ± 0.10
Brachial-ankle PWV (cm/s)	1587 ± 383	1783 ± 354*	1887 ± 387**
Ca (mmol/l)	2.30 ± 0.19	2.31 ± 0.10	2.33 ± 0.11
IP (mmol/l)	1.12 ± 0.20	1.05 ± 0.16	1.09 ± 0.16
ALP (IU/l)	233 ± 57	246 ± 52	228 ± 60
BNP (pg/ml)	17.8 ± 21.8	28.5 ± 38.0	33.2 ± 32.8*
Osteopontin (ng/ml)	299 ± 137	325 ± 117	375 ± 187*
Osteoprotegerin (pg/ml)	77.8 ± 34.3	87.1 ± 33.9	96.9 ± 43.3*

Data are expressed as *n* (%) or means ± SD. D, diet; OHD, oral hypoglycemic drugs; I, insulin.
* $p < 0.05$.
** $p < 0.01$.
*** $p < 0.001$ vs. the lowest group.
† $p < 0.05$ vs. the intermediate group.

Table 3 – Stepwise multiple regression analyses of the association in diabetic patients of log (CACS + 1) and carotid mean-IMT with 12 possible risk factors for atherosclerosis, two medications and two bone-related peptides.

	log(CACS + 1)		Carotid mean-IMT	
	β-value	F-value	β-value	F-value
Age	0.038	17.198	0.006	7.821
Duration of diabetes	0.024	4.821	–	0.385
FPG	–	0.763	–	0.980
HbA1c	–	0.053	–	0.088
TC	–	0.238	–	0.356
HDL-C	–	1.372	–	0.006
TGs	–	3.039	–	0.715
Use of statins	–	2.430	–	3.709
sBP	–	3.474	0.004	9.378
dBP	–	2.390	–	0.577
Use of ACEI or ARB	–	1.052	–	0.002
Smoking habit	–	2.342	–	0.485
Micro- or macroalbuminuria	–	0.700	–	0.164
eGFR	–	0.561	–	0.812
Osteopontin	0.001	6.302	0.001	5.177
Osteoprotegerin	–	1.487	0.001	5.708
r^2	0.215 ($p < 0.0001$)		0.203 ($p < 0.0001$)	

The *F*-value was set at 4.0 at each step.

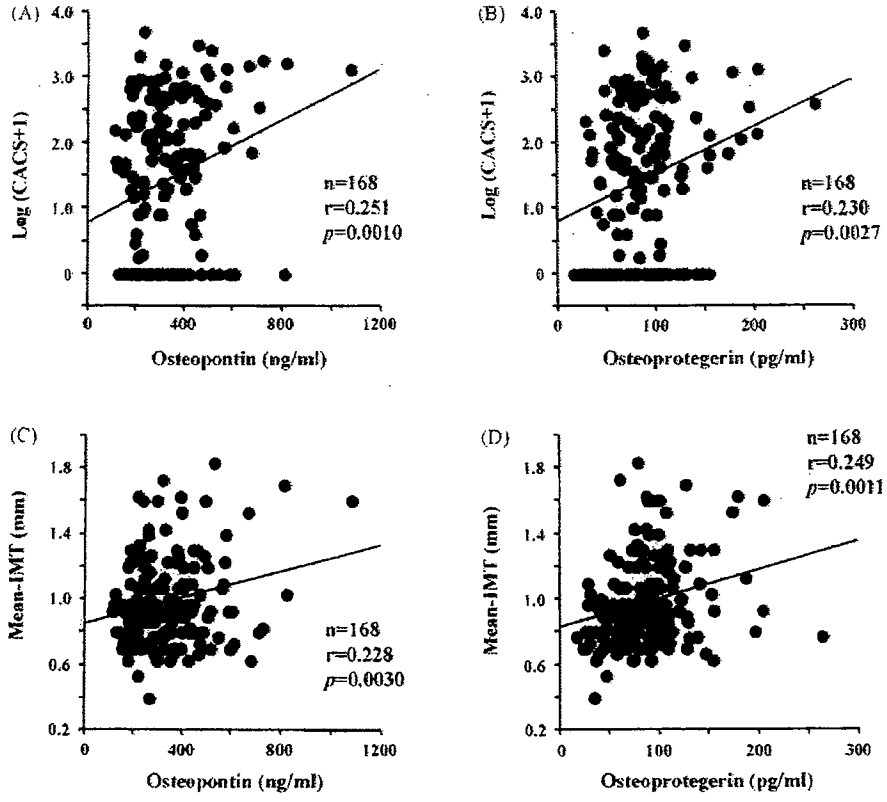

Fig. 2 – Simple linear regression analyses between coronary artery calcium score (CACS) (A and B) or mean value of intima-media thickness (mean-IMT) in the common carotid arteries (C and D) and plasma concentrations of osteopontin or osteoprotegerin in type 2 diabetic patients.

$P < 0.0001$) and those of mean-IMT were age, sBP, osteopontin and osteoprotegerin ($r^2 = 0.203$, $p < 0.0001$) in diabetic patients.

4. Discussion

In this study, diabetic patients with no clinical history of cerebrovascular disease, CAD, or peripheral artery occlusive disease had higher carotid IMT and coronary artery calcification than those in non-diabetic subjects, while plasma levels of the bone-related peptides osteopontin and osteoprotegerin were similar in the two groups. It has been reported that circulating levels of osteopontin [17] and osteoprotegerin [18] are higher in patients with 2- or 3-vessel disease, but are similar in patients with 1-vessel disease compared to those in patients without CAD assessed by coronary angiography. These results indicate that circulating levels of these molecules are elevated in individuals with severe atherosclerosis. Our present data show a positive correlation between coronary artery calcification and carotid IMT in diabetic patients, indicating that vascular calcification is frequently accompanied by intima-media thickening, and that these atherosclerotic features contribute to the stability of atherosclerotic plaques. Three distinct types of VSMCs, contractile, synthetic and calcifying, are found in the vessel wall [34]. The main function of contractile VSMCs is regulation of vascular tonus by contraction or relaxation, and a variety of inflammatory mediators can regulate differentiation of these cells. The responses of calcifying and synthetic VSMCs to chronic vascular inflammation contribute to the stability of atherosclerotic plaques [35,36]. Macrophage derived proinflammatory cytokine tumor necrosis factor-alpha is responsible for the induction of osteoblastic differentiation in VSMCs required to mineralize extracellular matrix [37] as well as for migration of VSMCs into the intimal layer that is followed by proliferation and secretion of extracellular matrix [38].

In this study, to compare the clinical characteristics of diabetic patients with coronary artery calcification, they were grouped into tertiles according to their CACS levels. Diabetic patients with the highest scores showed the highest age, duration of diabetes, systolic blood pressure, use of RAS inhibitors, frequency of retinopathy, carotid IMT, arterial stiffness and circulating levels of BNP, osteopontin and osteoprotegerin and the lowest kidney function among the groups. Our data demonstrate that both coronary artery calcification and carotid IMT are positively correlated with circulating levels of the bone-related peptides osteopontin and osteoprotegerin in diabetic patients. These findings suggest that elevation of circulating osteopontin and osteoprotegerin concentrations reflects an active calcifying process, and that these molecules act as vascular calcification inhibitors [12,15,16] and increase intima-media thickness, which promotes stability of

atherosclerotic plaques in diabetic patients. Multivariate analyses show that the significant independent determinants of coronary artery calcification are age, duration of diabetes and osteopontin and those of carotid IMT are age, hypertension, osteopontin and osteoprotegerin in diabetic patients. It is now recognized that age [39,40], hypertension [41,42] and type 2 diabetes [8,43] are important risk factors for both coronary artery calcification and carotid IMT. Our data indicate that bone-related peptides are involved in the pathogenesis of atherosclerosis in type 2 diabetic patients.

It has been reported that administration of RAS inhibitors or statins can decrease the progression of coronary artery calcification [23,25] and carotid IMT [24,26]. In addition, ARB can reduce osteoprotegerin secretion from carotid endarterectomy samples taken from stroke patients [9]. Administration of statins can also reduce plasma levels of osteopontin in patients with hypercholesterolemia [44] and those of osteoprotegerin in patients with type 2 diabetes [45]. However, our multivariate analyses show that use of these medications is not an independent predictor of vascular calcification or intima-media thickening in diabetic patients.

Our study has some limitations. Because the present study is a cross-sectional design, further prospective study is required to elucidate the role of bone-related peptides in the development of vascular calcification and intima-media thickening in type 2 diabetic patients. In addition, our data were obtained entirely in a Japanese population, so it remains to be established whether these findings can be generalized to other ethnicities.

In conclusion, we have demonstrated that vascular calcification is frequently accompanied by intima-media thickening in diabetic patients. The elevated plasma bone-related peptide osteopontin concentrations reflects an active calcifying process, and that the molecule may act as a vascular calcification inhibitor by increasing intima-media thickness, which promotes stability of atherosclerotic plaques in type 2 diabetic patients.

Conflict of interest

The authors declare that they have no conflict of interest.

Acknowledgments

This study was supported by Grant-in-Aid for Scientific Research on Priority Areas of Medical Genome Science from the Japanese Ministry of Science, Education, Sports, Culture and Technology and a Health and Labor Science Research Grant for Research on Human Genome and Tissue Engineering from the Japanese Ministry of Health, Labor and Welfare, and in part by the New Energy and Industrial Technology Development Organization Grant.

REFERENCES

[1] J. Kharlip, R. Naglieri, B.D. Mitchell, K.A. Ryan, T.W. Donner, Screening for silent coronary heart disease in type 2 diabetes: clinical application of American Diabetes Association guidelines, Diabetes Care 29 (2006) 692–694.

[2] L. Wexler, B. Brundage, J. Crouse, R. Detrano, V. Fuster, J. Maddahi, et al., Coronary artery calcification: pathophysiology, epidemiology, imaging methods, and clinical implications, a statement for hearth professionals from the American Heart Association. Writing Group, Circulation 94 (1996) 1175–1192.

[3] J.A. Rumberger, D.B. Simons, L.A. Fitzpatrick, P.F. Sheedy, R.S. Schwartz, Coronary artery calcium area by electron-beam computed tomography and coronary atherosclerotic plaque area. A histopathologic correlative study, Circulation 92 (1995) 2157–2162.

[4] J. Horiguchi, H. Yamamoto, Y. Akiyama, K. Murakawa, N. Hirai, K. Ito, Coronary artery calcium scoring using 16-MDCT and a retrospective ECG-gating reconstruction algorithm, Am. J. Roentgenol. 183 (2004) 103–108.

[5] A.S. Lachman, T.L. Spray, D.M. Kerwin, G.I. Shugoll, W.C. Roberts, Medial calcinosis of Mönckeberg. A review of the problem and a description of a patient with involvement of peripheral, visceral and coronary arteries, Am. J. Med. 63 (1977) 615–622.

[6] M. Hosoi, T. Sato, K. Yamagami, T. Hasegawa, T. Yamakita, M. Miyamoto, et al., Impact of diabetes on coronary stenosis and coronary artery calcification detected by electron-beam computed tomography in symptomatic patients, Diabetes Care 25 (2002) 696–701.

[7] N. Mitsuhashi, T. Onuma, S. Kubo, N. Takayanagi, M. Honda, R. Kawamori, Coronary artery disease and carotid artery intima-media thickness in Japanese type 2 diabetic patients, Diabetes Care 25 (2002) 1308–1312.

[8] S. Schurgin, S. Rich, T. Mazzone, Increased prevalence of significant coronary artery calcification in patients with diabetes, Diabetes Care 24 (2001) 335–338.

[9] J. Golledge, M. McCann, S. Mangan, A. Lam, M. Karan, Osteoprotegerin and osteopontin are expressed at high concentrations within symptomatic carotid atherosclerosis, Stroke 35 (2004) 1636–1641.

[10] L.A. Fitzpatrick, A. Severson, W.D. Edwards, R.T. Ingram, Diffuse calcification in human coronary arteries. Association of osteopontin with atherosclerosis, J. Clin. Invest. 94 (1994) 1597–1604.

[11] E.R. O'Brien, M.R. Garvin, D.K. Stewart, T. Hinohara, J.B. Simpson, S.M. Schwartz, et al., Osteopontin is synthesized by macrophage, smooth muscle, and endothelial cells in primary and restenotic human coronary atherosclerotic plaques, Arterioscler. Thromb. 14 (1994) 1648–1656.

[12] C.M. Giachelli, M.Y. Speer, X. Li, R.M. Rajachar, H. Yang, Regulation of vascular calcification: roles of phosphate and osteopontin, Circ. Res. 96 (2005) 717–722.

[13] L.C. Hofbauer, C. Shui, B.L. Riggs, C.R. Dunstan, T.C. Spelsberg, T. O'Brien, et al., Effects of immunosuppressants on receptor activator of NF-kappaB ligand and osteoprotegerin production by human osteoblastic and coronary artery smooth muscle cells, Biochem. Biophys. Res. Commun. 280 (2001) 334–339.

[14] P. Collin-Osdoby, L. Rothe, F. Anderson, M. Nelson, W. Maloney, P. Osdoby, Receptor activator of NF-kappa B and osteoprotegerin expression by human microvascular endothelial cells, regulation by inflammatory cytokines, and role in human osteoclastogenesis, J. Biol. Chem. 276 (2001) 20659–20672.

[15] W.S. Simonet, D.L. Lacey, C.R. Dunstan, M. Kelley, M.S. Chang, R. Lüthy, et al., Osteoprotegerin: a novel secreted protein involved in the regulation of bone density, Cell 89 (1997) 309–319.

[16] P.A. Price, H.H. June, J.R. Buckley, M.K. Williamson, Osteoprotegerin inhibits artery calcification induced by

warfarin and by vitamin D, Arterioscler. Thromb. Vasc. Biol. 21 (2001) 1610–1616.
[17] R. Ohmori, Y. Momiyama, H. Taniguchi, R. Takahashi, M. Kusuhara, H. Nakamura, et al., Plasma osteopontin levels are associated with the presence and extent of coronary artery disease, Atherosclerosis 170 (2003) 333–337.
[18] S. Jono, Y. Ikari, A. Shioi, K. Mori, T. Miki, K. Hara, et al., Serum osteoprotegerin levels are associated with the presence and severity of coronary artery disease, Circulation 106 (2002) 1192–1194.
[19] P. Minoretti, C. Falcone, M. Calcagnino, E. Emanuele, M.P. Buzzi, E. Coen, et al., Prognostic significance of plasma osteopontin levels in patients with chronic stable angina, Eur. Heart J. 27 (2006) 802–807.
[20] D.V. Anand, A. Lahiri, E. Lim, D. Hopkins, R. Corder, The relationship between plasma osteoprotegerin levels and coronary artery calcification in uncomplicated type 2 diabetic subjects, J. Am. Coll. Cardiol. 47 (2006) 1850–1857.
[21] A. Avignon, A. Sultan, C. Piot, S. Elaerts, J.P. Cristol, A.M. Dupuy, Osteoprotegerin is associated with silent coronary artery disease in high-risk but asymptomatic type 2 diabetic patients, Diabetes Care 28 (2005) 2176–2180.
[22] T.J. Orchard, D.E. Strandness Jr., Assessment of peripheral vascular disease in diabetes. Report and recommendations of an international workshop sponsored by the American Heart Association and the American Diabetes Association 18-20 September 1992, New Orleans, Louisiana, Diabetes Care 16 (1993) 1199–1209.
[23] D.M. Maahs, J.K. Snell-Bergeon, G.L. Kinney, R.P. Wadwa, S. Garg, L.G. Ogden, et al., ACE-I/ARB treatment in type 1 diabetes patients with albuminuria is associated with lower odds of progression of coronary artery calcification, J. Diabetes Complications 21 (2007) 273–279.
[24] N. Hosomi, K. Mizushige, H. Ohyama, T. Takahashi, M. Kitadai, Y. Hatanaka, et al., Angiotensin-converting enzyme inhibition with enalapril slows progressive intima-media thickening of the common carotid artery in patients with non-insulin-dependent diabetes mellitus, Stroke 32 (2001) 1539–1545.
[25] S. Achenbach, D. Ropers, K. Pohle, A. Leber, C. Thilo, A. Knez, et al., Influence of lipid-lowering therapy on the progression of coronary artery calcification: a prospective evaluation, Circulation 106 (2002) 1077–1082.
[26] A.J. Taylor, S.M. Kent, P.J. Flaherty, L.C. Coyle, T.T. Markwood, M.N. Vernalis, ARBITER: Arterial Biology for the Investigation of the Treatment Effects of Reducing Cholesterol: a randomized trial comparing the effects of atrovastatin and pravastatin on carotid intima medial thickness, Circulation 106 (2002) 2055–2060.
[27] K.G. Alberti, P.Z. Zimmet, Definition, diagnosis and classification of dibetes mellitus and its complications. Part 1: diagnosis and classification of diabetes mellitus provisional report of a WHO consultation, Diabet. Med. 15 (1998) 539–553.
[28] A. Yamashina, H. Tomiyama, K. Takeda, H. Tsuda, T. Arai, K. Hirose, et al., Validity, reproducibility, and clinical significance of noninvasive brachial-ankle pulse wave velocity measurement, Hypertens. Res. 25 (2002) 359–364.
[29] A.J. Boulton, A.I. Vinik, J.C. Arezzo, V. Bril, E.L. Feldman, R. Freeman, et al., Diabetic neuropathies: a statement by the American Diabetes Association, Diabetes Care 28 (2005) 956–962.
[30] American Diabetes Association, Standards of medical care in diabetes – 2008, Diabetes Care 31 (2008) S12–S54.
[31] E. Imai, M. Horio, K. Nitta, K. Yamagata, K. Iseki, S. Hara, et al., Estimation of glomerular filtration rate by the MDRD study equation modified for Japanese patients with chronic kidney disease, Clin. Exp. Nephrol. 11 (2007) 41–50.
[32] National Kidney Foundation, K/DOQI clinical practice guidelines for chronic kidney disease: evaluation, classification, and stratification, Am. J. Kidney Dis. 39 (Suppl. 1) (2002) S46–S64.
[33] A.S. Agatston, W.R. Janowitz, F.J. Hildner, N.R. Zusmer, M. Viamonte Jr., R. Detrano, Quantification of coronary artery calcium using ultrafast computed tomography, J. Am. Coll. Cardiol. 15 (1990) 827–832.
[34] A. Trion, A. van der Laarse, Vascular smooth muscle cells and calcification in atherosclerosis, Am. Heart J. 147 (2004) 808–814.
[35] A.H. Kragel, S.G. Reddy, J.T. Wittes, W.C. Roberts, Morphometric analysis of the composition of atherosclerotic plaques in the four major epicardial coronary arteries in acute myocardial infarction and in sudden coronary death, Circulation 80 (1989) 1747–1756.
[36] J. Shemesh, S. Apter, Y. Itzchak, M. Motro, Coronary calcification compared in patients with acute versus in those with chronic coronary events by using dual-sector spiral CT, Radiology 226 (2003) 483–488.
[37] A. Shioi, M. Katagi, Y. Okuno, K. Mori, S. Jono, H. Koyama, et al., Induction of bone-type alkaline phosphatase in human vascular smooth muscle cells: roles of tumor necrosis factor-alpha and oncostatin M derived from macrophages, Circ. Res. 91 (2002) 9–16.
[38] S. Jovinge, A. Hultgårdh-Nilsson, J. Regnström, J. Nilsson, Tumor necrosis factor-alpha activates smooth muscle cell migration in culture and is expressed in the balloon-injured rat aorta, Arterioscler. Thromb. Vasc. Biol. 17 (1997) 490–497.
[39] W.R. Janowitz, A.S. Agatston, G. Kaplan, M. Viamonte Jr., Differences in prevalence and extent of coronary artery calcium detected by ultrafast computed tomography in asymptomatic men and women, Am. J. Cardiol. 72 (1993) 247–254.
[40] Y. Yamasaki, R. Kawamori, H. Matsushima, H. Nishizawa, M. Kodama, Y. Kajimoto, et al., Atherosclerosis in carotid artery of young IDDM patients monitored by ultrasound high-resolution B-mode imaging, Diabetes 43 (1994) 634–639.
[41] J.L. Megnien, A. Simon, M. Lemariey, M.C. Plainfossé, J. Levenson, Hypertension promotes coronary calcium deposit in asymptomatic men, Hypertension 27 (1996) 949–954.
[42] M. Puato, P. Palatini, M. Zanardo, F. Dorigatti, C. Tirrito, et al., Increase in carotid intima-media thickness in grade 1 hypertensive subjects: white-coat versus sustained hypertension, Hypertension 51 (2008) 1300–1305.
[43] Y. Yamasaki, M. Kodama, H. Nishizawa, K. Sakamoto, M. Matsuhisa, Y. Kajimoto, et al., Carotid intima-media thickness in Japanese type 2 diabetic subjects: predictors of progression and relationship with incident coronary heart disease, Diabetes Care 23 (2000) 1310–1315.
[44] N. Tanaka, Y. Momiyama, R. Ohmori, A. Yonemura, M. Ayaori, et al., Effect of atorvastatin on plasma osteopontin levels in patients with hypercholesterolemia, Arterioscler. Thromb. Vasc. Biol. 26 (2006) e129–130.
[45] B. Nellemann, L.C. Gormsen, J. Dollerup, O. Schmitz, C.E. Mogensen, L.M. Rasmussen, et al., Simvastatin reduces plasma osteoprotegerin in type 2 diabetic patients with microalbuminuria, Diabetes Care 30 (2007) 3122–3124.

Sonographic Evaluation of the Median Nerve in Diabetic Patients

Comparison With Nerve Conduction Studies

Tsuneo Watanabe, MT, Hiroyasu Ito, MD, PhD, Ayako Morita, MT, Yuriko Uno, MT, Takashi Nishimura, MT, Harumi Kawase, PhD, Yoshihiro Kato, MD, PhD, Toshio Matsuoka, PhD, Jun Takeda, MD, PhD, Mitsuru Seishima, MD, PhD

Objective. Diabetes mellitus is becoming a major cause of premature disability in Japan, and peripheral neuropathy is a common complication of diabetes. The aim of this study was to evaluate the relationship between the results of nerve conduction studies (NCS) and the size of the nerve determined by sonography in diabetic patients. ***Methods.*** Twenty diabetic patients (mean age ± SD, 57.1 ± 13.6 years) and 20 healthy volunteers (mean, 61.1 ± 8.9 years) were enrolled in this study. Patients' wrists that had symptoms of carpal tunnel syndrome were not included in the study; those that were included had negative Phalen test results. We then divided the patients into 2 groups (patients with and without diabetic symmetric polyneuropathy [DPN]). The cross-sectional area (CSA) was measured in the carpal tunnel 5 cm proximal to the wrist and elbow joint of the median nerve. ***Results.*** There was a significant increase in the CSA in patients with DPN in the carpal tunnel compared with the control participants ($P < .01$) and patients without DPN ($P < .01$). The CSA in the carpal tunnel showed a significant correlation with the motor nerve conduction velocity ($r = -0.473$). ***Conclusions.*** The CSA of the median nerve in the carpal tunnel of patients with DPN is greater than that in patients without DPN and healthy individuals and correlates with NCS. ***Key words:*** cross-sectional area; diabetes mellitus; median nerve measurement; neuropathy; sonography.

Abbreviations
CSA, cross-sectional area; CTS, carpal tunnel syndrome; DPN, diabetic symmetric polyneuropathy; MCV, motor nerve conduction velocity; NCS, nerve conduction studies

Received December 16, 2008, from the Clinical Laboratory Section, Gifu University Hospital, Gifu, Japan (T.W., A.M., Y.U., T.N., H.K.); and Department of Sports Medicine and Sports Science (T.W., Y.K., T.M.), Division of Molecule and Structure Research, Field of Medical Sciences (J.T.), and Department of Informative Clinical Medicine (H.I., M.S.), Gifu University Graduate School of Medicine, Gifu, Japan. Revision requested January 7, 2009. Revised manuscript accepted for publication January 14, 2009.

We thank Hitachi Medical Corporation (Tokyo, Japan) for equipment support.

Address correspondence to Hiroyasu Ito, MD, PhD, Department of Informative Clinical Medicine, Gifu University Graduate School of Medicine, 1-1 Yanagido, Gifu 501-1194, Japan.
E-mail: hito@gifu-u.ac.jp

CME *Article includes CME test*

Nowadays, the number of diabetic patients in Japan has increased and has reached 7 million, and it is estimated that 35% to 45% of diabetic patients have diabetic symmetric polyneuropathy (DPN). Advanced DPN causes serious complications, such as diabetic foot ulcers, gangrene, and Charcot joint, all of which worsen the quality of life in diabetic patients.[1] Therefore, early detection of nerve dysfunctions is important to provide appropriate care for patients with DPN.[2] The diagnosis of diabetic neuropathy is mainly based on the characteristic symptoms and confirmed by nerve conduction studies (NCS). Although imaging analyses for neuropathy have not been used for diagnosis, diagnostic ultrasound apparatuses with high resolution have been greatly improved, and the revelation of minute peripheral nerves by sonographic evaluation has become possible.[3] Recent studies using sonography for entrapment neuropathy such as carpal tunnel syndrome (CTS) have been reported.[3–7]

However, there have been a few reports of the sonographic depiction of DPN. The aim of this study was to evaluate the relationship between the results of NCS and the size of the nerve determined by sonography in diabetic patients.

Materials and Methods

Three type 1 and 17 type 2 diabetic patients were enrolled in this study at the Gifu University Hospital from October 2007 to February 2008 (13 male and 7 female; age range, 25–83 years; mean ± SD, 57.1 ± 13.6 years). For comparison, we recruited 20 healthy volunteers without diabetes mellitus or CTS. They were all male, ranging in age from 33 to 72 years (mean, 61.1 ± 8.9 years). Patients' wrists that had symptoms of carpal tunnel syndrome were not included in the study; those that were included had negative Phalen test results. We studied a total of 80 upper limbs in 40 participants who underwent sonography and NCS. Although many diagnostic criteria for DPN have been established, each item is unlikely to be easily examined in daily practice.[8] For the purpose of daily use, the Diabetic Neuropathy Study Group of Japan proposed simplified diagnostic criteria for DPN.[9] We divided the patients into 2 groups (patients with and without DPN) according to those diagnostic criteria.[9] The diagnostic criteria for DPN include the following: (1) diagnosis of diabetes mellitus and (2) exclusion of neuropathies other than diabetic neuropathy. The criteria should meet any 2 of the following 3 items: (1) sensory symptoms considered to be due to DPN, (2) a bilaterally decreased or absent ankle reflex, and (3) a decreased vibratory sensation in the bilateral medial malleoli. This study was approved by the Institutional Review Board of Gifu University Hospital, and informed consent was obtained from all participants.

Sonographic Examinations

Sonographic examinations were performed by 2 experienced sonographers, who were blinded to the participant's history and NCS results, using a 13- to 14-MHz linear array probe and a B-mode portable real-time apparatus (EUB-7500, Hitachi Medical Corporation, Tokyo, Japan; or ProSound Alpha 10, Aloka Co, Ltd, Tokyo, Japan). All examinations were performed with the participants in a supine position on a table. All examiners had a board-certified sonographer's license and more than 13 years of experience. The major axis, minor axis, and cross-sectional area (CSA) were measured in the carpal tunnel 5 cm proximal to the wrist and elbow joint of the median nerve. The CSA was calculated by the indirect method with the formula major axis × minor axis × π × 1/4 (square millimeters). The volar wrist crease and pisiform bone were used as initial external reference points and landmarks during scanning. Transverse and longitudinal sonograms of the median nerve at each position were recorded (Figure 1). When the median nerve showed a speckled pattern, the size of the nerve was assessed. Three sonographers also reviewed the recorded sonograms without knowledge of electrodiagnostic results based on size and shape.

Electrophysiologic Examinations

Routine NCS were performed with conventional procedures and a standard electromyography system (Neuropack MEB-2200, Nihon Kohden Corporation, Tokyo, Japan). All NCS were performed on both hands, and 2 sets of signals were measured by the method of Chino[10]: (1) the distal motor latency of the median nerve from the wrist joint to the thenar muscle and (2) the motor nerve conduction velocity (MCV) from the elbow to the wrist joint.

A plate-shaped surface electrode attached to the belly of the abductor pollicis brevis muscle was the pickup; the same type of electrode attached to the peripheral adherent part of the same muscle was the reference. A ground was placed on the palm area. The stimulating point at the wrist was placed between the 2 tendons of the flexor carpi radialis and the palmaris longus in the proximal part of the carpal tunnel. The distance between the stimulating point and the pickup electrode was set at 7 cm. A supramaximal nerve stimulus was applied, and the time from the stimulus in the periphery to the onset of the evoked response was taken as the distal motor latency. A proximal stimulating point was then set at the elbow just medial to the palpable brachial artery, and the MCV in the forearm was obtained by calculation from the distance of 2 stimulating points and the difference of each response time. All of the exam-

inations were performed in a room with an ambient temperature of 25°C. The skin surface temperature was in all cases between 31°C and 33°C.

Statistical Analysis

The Kruskal-Wallis test and Mann-Whitney *U* test were used to compare the data in the 3 groups and between 2 groups, respectively.

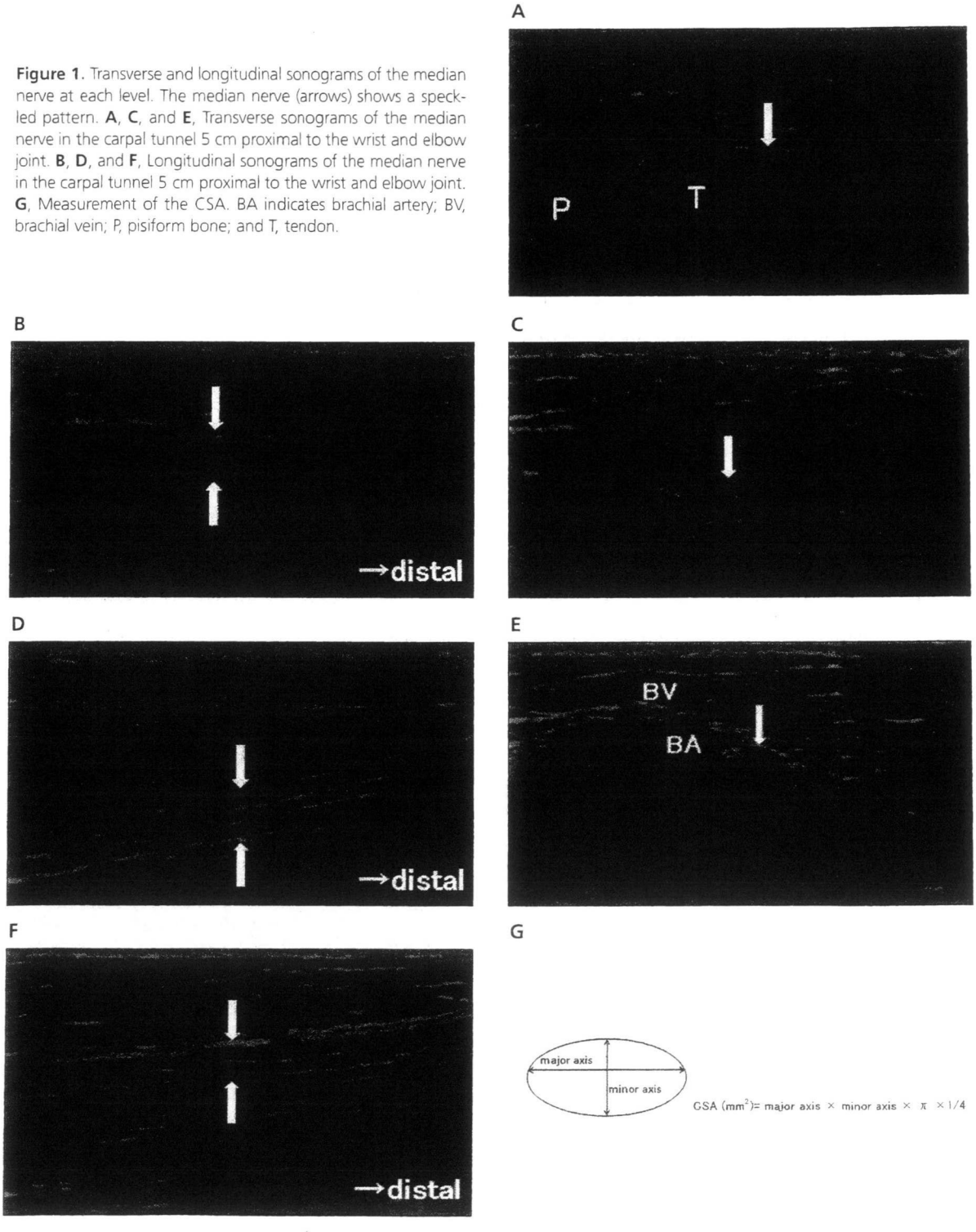

Figure 1. Transverse and longitudinal sonograms of the median nerve at each level. The median nerve (arrows) shows a speckled pattern. **A**, **C**, and **E**, Transverse sonograms of the median nerve in the carpal tunnel 5 cm proximal to the wrist and elbow joint. **B**, **D**, and **F**, Longitudinal sonograms of the median nerve in the carpal tunnel 5 cm proximal to the wrist and elbow joint. **G**, Measurement of the CSA. BA indicates brachial artery; BV, brachial vein; P, pisiform bone; and T, tendon.

inations were performed in a room with an ambient temperature of 25°C. The skin surface temperature was in all cases between 31°C and 33°C.

Statistical Analysis

The Kruskal-Wallis test and Mann-Whitney *U* test were used to compare the data in the 3 groups and between 2 groups, respectively.

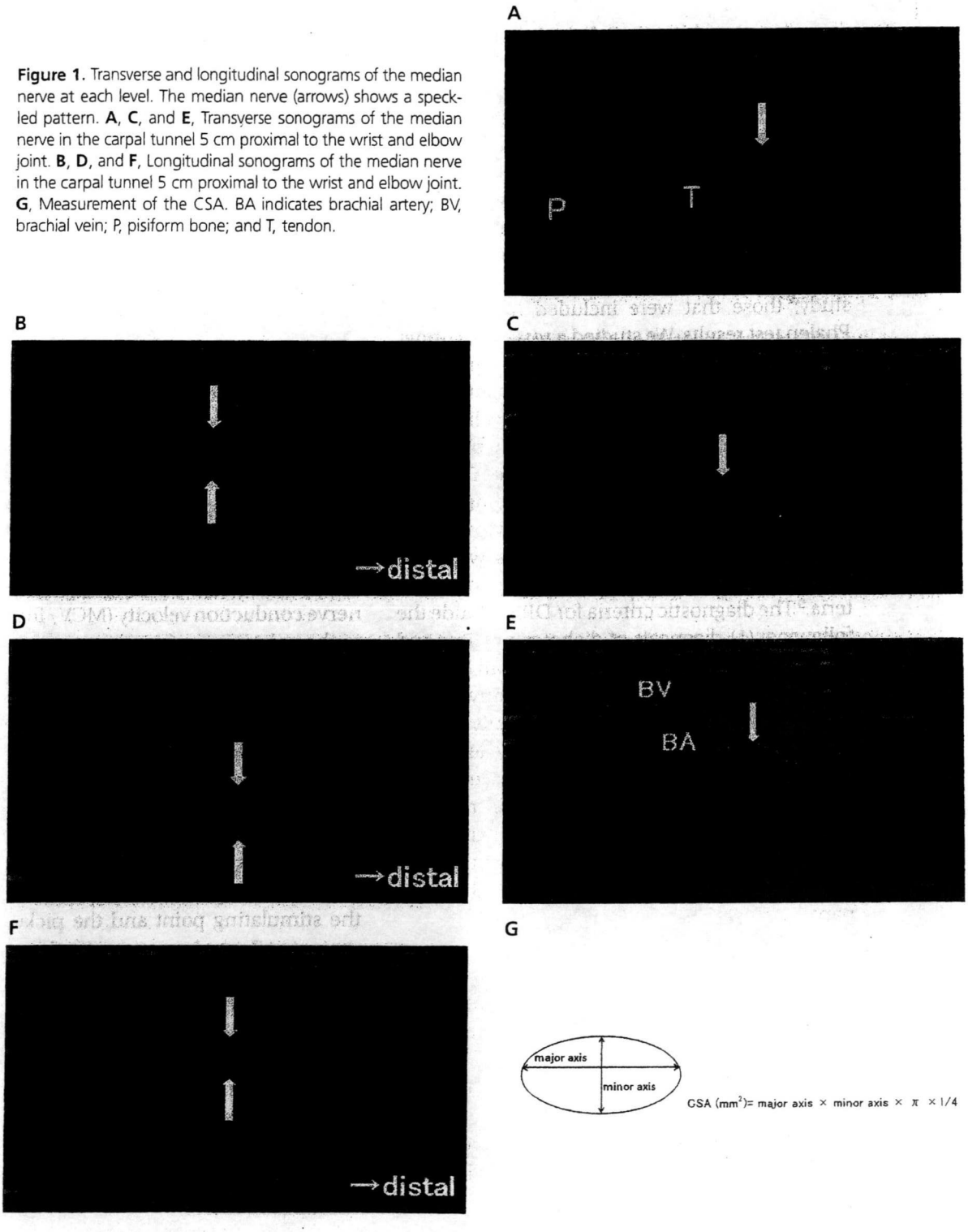

Figure 1. Transverse and longitudinal sonograms of the median nerve at each level. The median nerve (arrows) shows a speckled pattern. **A**, **C**, and **E**, Transverse sonograms of the median nerve in the carpal tunnel 5 cm proximal to the wrist and elbow joint. **B**, **D**, and **F**, Longitudinal sonograms of the median nerve in the carpal tunnel 5 cm proximal to the wrist and elbow joint. **G**, Measurement of the CSA. BA indicates brachial artery; BV, brachial vein; P, pisiform bone; and T, tendon.

To correlate the nerve CSA with other parameters, the Pearson correlation coefficient test was used. The results obtained are given as mean ± SD, and statistical significance was assessed at $P < .05$.

Results

Detailed demographic data for the patients with diabetes mellitus and control participants are shown in Table 1. There were no significant differences in age, height, weight, body mass index, and body surface area between control participants and diabetic patients. The sonographic and NCS results for the diabetic patients and control participants are shown in Table 2. The CSAs in the patients without DPN were 9 ± 2 mm^2 in the carpal tunnel, 7.1 ± 1.6 mm^2 in the wrist, and 7.4 ± 3.2 mm^2 in the elbow joint; those in the patients with DPN were 13.5 ± 2.8 mm^2 in the carpal tunnel, 9.1 ± 2.7 mm^2 in the wrist, and 7.2 ± 2.6 mm^2 in the elbow joint; and those in the control participants were 9 ± 1.5 mm^2 in the carpal tunnel, 7.4 ± 1.4 mm^2 in the wrist, and 7.5 ± 1.8 mm^2 in the elbow joint. There was a significant increase in the CSA in patients with DPN in the carpal tunnel compared with the control participants ($P < .01$) and diabetic patients without DPN ($P < .01$). Sonograms of diabetic patients and the control participants are shown in Figure 2.

There was a significant decrease in the MCV in patients with DPN compared with the control participants ($P < .01$) and patients without DPN ($P < .01$). The CSA in the carpal tunnel showed a significant correlation with latency ($r = 0.364$; $P < .01$; Figure 3) and the MCV ($r = -0.473$; $P < .001$; Figure 4). In the wrist and elbow joint, no significant relationship was found between the size of the CSA and any NCS.

Table 1. Characteristics of the Study Participants

Variable	Control Participants	Diabetic Patients With DPN	Diabetic Patients Without DPN
n	20	13	7
Sex, male/female	20/0	8/5	5/2
Age, y[a]	61.1 ± 8.9	55.3 ± 12.4	60.9 ± 12.4
Height, cm[a]	167.1 ± 4.9	162.7 ± 8.4	165.6 ± 5.6
Weight, kg[a]	64.7 ± 8.6	67.9 ± 22.8	64.9 ± 8.5
Body mass index, %[a]	23.2 ± 2.6	25.7 ± 6.7	23.8 ± 2.8
Body surface area, m^2[a]	1.73 ± 0.12	1.71 ± 0.26	1.71 ± 0.12
Type, n (%)	NA	1: 23.1 (3/13); 2: 76.9 (10/13)	1: 0 (0/7); 2: 100 (7/7)
Duration, y[a]	NA	9.2 ± 8.3	17.7 ± 12.7
Hemoglobin A_{1c}, %[a]	NA	9 ± 2.5	8.7 ± 1.3

NA indicates not applicable.
[a]Values are mean ± SD.

Table 2. Sonographic and Electrophysiologic Measurements in the Study Participants

Parameter	Control Participants (n = 40 Upper Limbs)	Diabetic Patients Without DPN (n = 26 Upper Limbs)	Diabetic Patients With DPN (n = 14 Upper Limbs)	*P* Among Groups, Kruskal-Wallis
Sonographic measurements (CSA)				
Level of carpal tunnel, mm^2	9 ± 1.5	9 ± 2	13.5 ± 2.8[a,b]	<.001
Level of distal 5 cm from wrist, mm^2	7.4 ± 1.4	7.1 ± 1.6	9.1 ± 2.7[c]	<.001
Level of elbow joint, mm^2	7.5 ± 1.8	7.4 ± 3.2	7.2 ± 2.6	NS
Electrophysiologic measurements				
Latency, ms	3.8 ± 0.5	3.9 ± 0.9	4.8 ± 1.5[d,e]	NS
MCV, m/s	52.8 ± 3.7	53 ± 5.1	46.8 ± 3.7[a,b]	<.001

Values are mean ± SD. NS indicates not significant ($P > .05$).
[a]$P < .001$ versus control participants by the Mann-Whitney *U* test.
[b]$P < .001$ versus diabetic patients without DPN by the Mann-Whitney *U* test.
[c]$P < .01$ versus diabetic patients without DPN by the Mann-Whitney *U* test.
[d]$P < .05$ versus control participants by the Mann-Whitney *U* test.
[e]$P < .05$ versus diabetic patients without DPN by the Mann-Whitney *U* test.

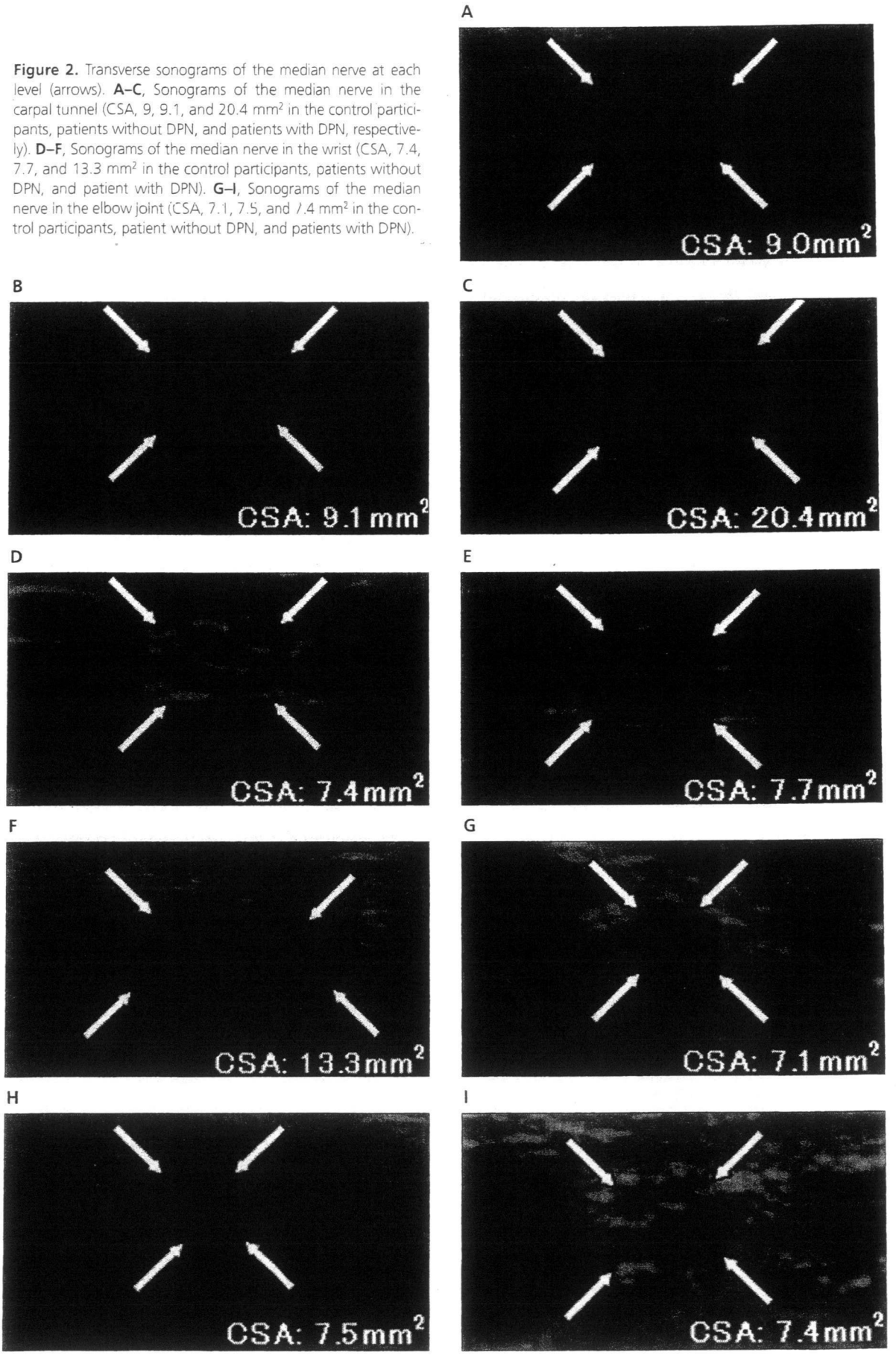

Figure 2. Transverse sonograms of the median nerve at each level (arrows). **A–C**, Sonograms of the median nerve in the carpal tunnel (CSA, 9, 9.1, and 20.4 mm^2 in the control participants, patients without DPN, and patients with DPN, respectively). **D–F**, Sonograms of the median nerve in the wrist (CSA, 7.4, 7.7, and 13.3 mm^2 in the control participants, patients without DPN, and patient with DPN). **G–I**, Sonograms of the median nerve in the elbow joint (CSA, 7.1, 7.5, and 7.4 mm^2 in the control participants, patient without DPN, and patients with DPN).

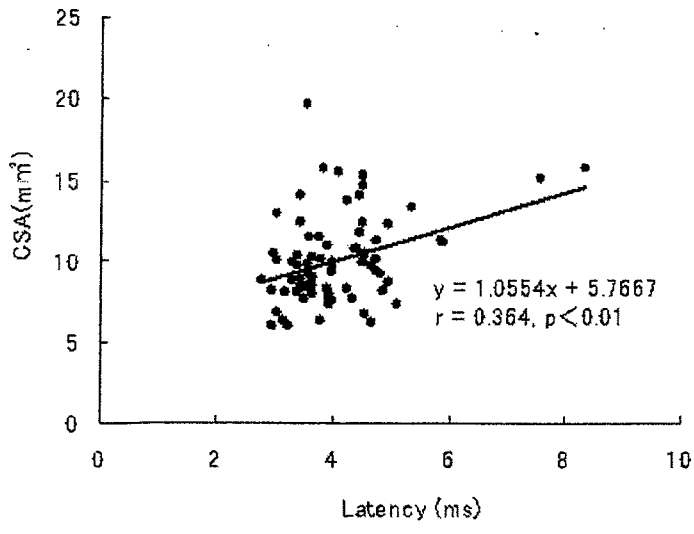

Figure 3. Correlation of CSA and latency. The CSA in the carpal tunnel showed a significant correlation with latency ($r = 0.364$; $P < .01$).

Discussion

Diabetes mellitus is becoming a major cause of premature disability in Japan, and peripheral neuropathy is a common complication of diabetes.[11] The diagnosis of diabetic neuropathy is mainly based on the characteristic symptoms and can be confirmed with NCS.[11–14] However, NCS are time-consuming, slightly invasive, and generally not well tolerated for repeated evaluations.[15] On the other hand, sonographic studies recently have been reported for evaluation of patients with entrapment disease such as CTS. They may be useful alternatives to NCS with high sensitivity and specificity.[3–7] Sonographic measurements of the nerve CSA include 2 methods: the indirect method (ellipsoid formula) and the direct method (tracing). Recently, Alemán et al[16] reported that sonography for median nerve CSA measurements was reproducible by either the tracing or indirect method when a standardized sonographic examination protocol was used. Another recent study recognized that multilevel assessment for diagnosis of CTS was more accurate than evaluation at a single level when using sonography because there was an individual variation in the swollen part of the median nerve in patients with CTS.[5] Consequently, we used the easier indirect method for the examination and measured at the site of 3 established portions of the forearm.

Conventional motor and sensory NCS have been widely used to diagnose DPN.[17–24] The symptoms of DPN are recognized to appear bilaterally from the soles or toes of the feet. Thus, NCS in the lower limbs should be more suitable for assessing the severity of DPN. However, NCS in the lower limbs are time-consuming, and action potentials in the lower limbs sometimes cannot be evoked in patients with advanced DPN. Some previous studies reported that MCV slowing in the upper limbs was similar to that in the lower limbs of diabetic patients.[25,26] In addition, the skin temperature and humidity easily affect the sensory nerve conduction velocity at the time of measurement, so it is often impossible to measure. Mizumoto et al[27] reported that they chose instead to look at the distal motor latency and MCV because the sensory nerve conduction velocity was not measurable in many hands and therefore appeared to be an unsuitable parameter. Because of these reasons, we performed motor nerve conduction studies only in the upper limbs. Of course, an NCS of the lower limbs might be a more sensitive method for detecting DPN.

In the cross-sectional study of diabetic neuropathy reported by Dyck et al,[13] the polyneuropathy found to be the most common form of diabetic neuropathy was DPN, followed by CTS. It is well

Figure 4. Correlation of CSA and MCV. The CSA in the carpal tunnel showed a significant correlation with the MCV ($r = -0.473$; $P < .001$).